Time-Resolved X-Ray Spectroscopy of Nucleobases and Their Thionated Analogs

Dennis Mayer*[1], Fabiano Lever [1], Markus Gühr* [1,2]

[1]. Deutsches Elektronen-Synchrotron DESY, Notkestr. 85, 22607 Hamburg, Germany, [2]. Institute of Physical Chemistry, University of Hamburg, Grindelallee 117, 20146 Hamburg, Germany

* Corresponding author e-mail: dennis.mayer@desy.de (Dennis Mayer), markus.guehr@desy.de (Markus Gühr)

ABSTRACT

The photoinduced relaxation dynamics of nucleobases and their thionated analogs have been investigated extensively over the past decades motivated by their crucial role in organisms and their application in medical and biochemical research and treatment. Most of these studies focused on the spectroscopy of valence electrons and fragmentation. The advent of ultrashort x-ray laser sources such as free-electron lasers, however, opens new opportunities for studying the ultrafast molecular relaxation dynamics utilizing the site- and element-selectivity of x-rays. In this review we want to summarize ultrafast experiments on thymine and 2-thiouracil performed at free-electron lasers. We performed time-resolved x-ray absorption spectroscopy at the oxygen K-edge after UV excitation of thymine. In addition, we investigated the excited state dynamics of 2-tUra via x-ray photoelectron spectroscopy at sulfur. For these methods, we show a strong sensitivity to the electronic state or charge distribution, respectively. We also performed time-resolved Auger-Meitner spectroscopy, which shows spectral shifts associated to internuclear distances close to the probed site. We discuss the complementary aspects of time-resolved x-ray spectroscopy techniques compared to optical and UV spectroscopy for the investigation of ultrafast relaxation processes.

INTRODUCTION

Nucleobases and their thionated analogs play a crucial role in life. As core constituents of the DNA, nucleobases encode the genetic information and participate in different parts in metabolism. Nucleobases exhibit large UV absorption cross sections. In DNA, such UV-induced excitations can lead to the formation of intrastrand dimers between neighboring nucleobase pairs [1]. These UV-induced lesions affect the reproduction of DNA and can eventually lead to mutations and cell death. However, the low quantum efficiency for these processes limits the rate of formation of such dimers. Already in isolated nucleobases one observes a competing relaxation mechanism: ultrafast relaxation from the photoexcited state back into the ground state provides a protective channel [2,3] by dissipating the photoexcitation as heat. For pyrimidine lesions, time-resolved UV pump-infrared probe studies show the complex interplay that ground-state relaxation and dimerization play in photoprotection [4].

Upon thionation, i.e. the substitution of oxygen atoms with sulfur, the photophysics and photochemistry of nucleobases significantly changes. Strong redshifts in the absorption spectrum allow thionucleobases to absorb in the UV-B or even UV-A spectral range. In combination with their structural similarity to canonical nucleobases, they find application medical biochemical research e.g., as biomarkers, but also as medication in immunosuppression or as antithyroid drug [5–8]. In contrast to their canonical counterparts, they efficiently relax into long-lived triplet states that promote intrastrand cross-linking or photolesions which can be exploited for photodynamic therapy [9]. However, these very same features make these molecules dangerous in their other forms of medication (immunosuppression) due to the abundance of UV-A in terrestrial sunlight. Apart from their medical and research applications, it is assumed that thionucleobases played a role in early biological structures [10–12].

A combination of ultrafast experiments and simulations have led to an increased understanding of the photoinduced dynamics of nucleobases and their thionated analogs [2,3,13–16]. Various experimental techniques have been used to investigate the electronic and nuclear dynamics and have been combined with extensive theoretical calculations to understand relaxation after UV excitation [14,15]. Conical intersections (CI) play a key role in the relaxation dynamics of these molecules [17,18]. These are regions in the potential energy landscape where the potential energy surfaces of two different electronic states approach each other and intersect. In these regions the Born-Oppenheimer approximation (BOA) breaks down. In short, the BOA allows to decouple electron and nuclear motion in quantum mechanical calculations as it assumes that the much lighter electrons can immediately react to any changes of the molecular geometry. However, as the energy gap between two PES decreases, the time scales of nuclear and electronic motion converge, coupling the two degrees of freedom. This allows the electronic wavepacket to release excess energy from optical excitations by changing molecular geometry and electronic state. Therefore, the shape and gradient of the PESs and which minimum can be reached fastest

have a large influence in the relaxation pathway. In general, relaxation via conical intersections often dominates over radiative deactivation channels as fluorescence happens on much slower timescales.

In many instances, the search for the exact relaxation pathways remains a struggle. Experimental techniques that focus on studying only the valence electrons often cannot distinguish between electronic and nuclear degrees of freedom and have difficulties to identify electronic states involved in the relaxation without expensive theoretical calculations. This might lead to the proposal of multiple relaxation pathways that are all compatible with experimental findings, as was the case for thymine [19,20].

With the evolution of x-ray free electron lasers over the past two decades, it became possible to investigate molecular dynamics from a completely different perspective using core-level electrons. FELs not only provide ultrafast, intense light pulses, but the high photon energies of hundreds to thousands of eV allow for probing highly localized core-level electrons inside the molecules. The element and site-selectivity that comes with the use of x-ray pulses allows for a systematical probe of different locations in the sample, and provides new information that allows to disentangle electronic and nuclear degrees of freedom, giving more direct insight into the relaxation dynamics of UV excited molecules. Nowadays, several FEL facilities offer the opportunity to study molecules and other materials with ultrafast x-ray light all over the world [21–28].

When studying the relaxation dynamics of molecules with x-rays, the usage of the gas phase comes with some advantages. First, the experiment can be often directly compared to theory. The simulation of isolated molecules can be accomplished at a higher level in approximation and, hence, a comparison is easier and faster. Second, the low density of gas-phase targets allows for different experimental techniques to be employed on the molecular problems and, hence, offers the possibility to create a more holistic picture for the problem. Excited-state absorption, which is commonly used in solution-phase, is more time consuming in gas-phase due to the low density. The detection of charged particles, i.e. electrons and ions, gives access to different ‘mapping’ of the molecular dynamics of observables. In contrast to optical transitions among molecular electronic states in time-resolved absorption, the dipole selection rules in photoelectron spectroscopy are less confining due to the availability of ionization continua of different angular momentum [29]. The detection of ions also allows to retrieve information on the nuclear geometry based on Coulomb explosion imaging [30–32]. In solution phase, ion detection is prohibitive and electrons can, depending on their energy, only be collected from a rather thin surface layer. In addition to it, depending on the elemental composition of the solvent, the SXR pulses are strongly absorbed in the solvent.

In this review we summarize our studies on thymine (Thy) and 2-thiouracil (2-tUra) performed at x-ray free-electron laser facilities over the past decade. We will start with a brief overview on the proposed relaxation pathways of both molecules based on the valence spectroscopy and simulations performed before. Subsequently, we discuss different methodological approaches in time-resolved x-ray spectroscopy for gas phase targets. We

start with x-ray absorption, which allows us to disentangle the different electronic states involved in the relaxation. Then, we continue with photoelectron spectroscopy which is to deduce the localized charge at the probed atom via the observation of the Excited State Chemical Shift (ESCS). At the end, we discuss what can be learned from the Auger-Meitner decay that follows the core-ionization of UV-excited molecules.

NON-ADIABATIC RELAXATION DYNAMICS OF THYMINE AND 2-THIOURACIL

In this section we briefly review relaxation pathways for thymine and 2-thiouracil as proposed by different theoretical studies. This is accompanied by a summary of experiments performed in both gas and solution phase for the respective molecules. However, this summary is limited to experiments that use IR, visible or (V)UV light as the (soft) x-ray spectroscopy will be discussed in later parts of this review.

The relaxation of molecules in the excited states is determined by the shape of their potential energy (hyper-)surfaces (PES) and in particular by the minima, saddle points, conical intersections and potential energy barriers which can affect the relaxation of the system. During radiationless relaxation, the nuclear wavepacket explores the PES by following the gradient towards lower energy, starting from the Frank-Condon region of the initially excited electronic state. This minimum energy path approach is a standard method to investigate the PES from a static perspective and to get an idea of possible reaction pathways and their time scales [33]. The role played by nonadiabatic coupling between states such as conical intersections is often studied with dynamical simulations such as semiclassical surface hopping or multiconfigurational time-dependent Hartree [34,35].

In experiments, nucleobases have shown weak fluorescence yields after optical excitation [36]. This indicates that non-radiative deactivation mechanisms dominate. Theoretical studies describing possible pathways are summarized in ref [16]. In short, the excitation with UV light populates a ππ* state in these molecules. nπ* states, which sometimes are lower in energy, show weak oscillator strength for optical excitations due to the lone pair orbital n involved. However, conical intersections between these states and the ground state, often in the vicinity of the respective minima, facilitate non-radiative transitions with femtosecond to picosecond lifetimes. While tautomerism can have an effect on the relaxation dynamics of the molecule, pyrimidine-based nucleobases uracil and thymine, show negligible tautomerism even at high temperatures [37,38].

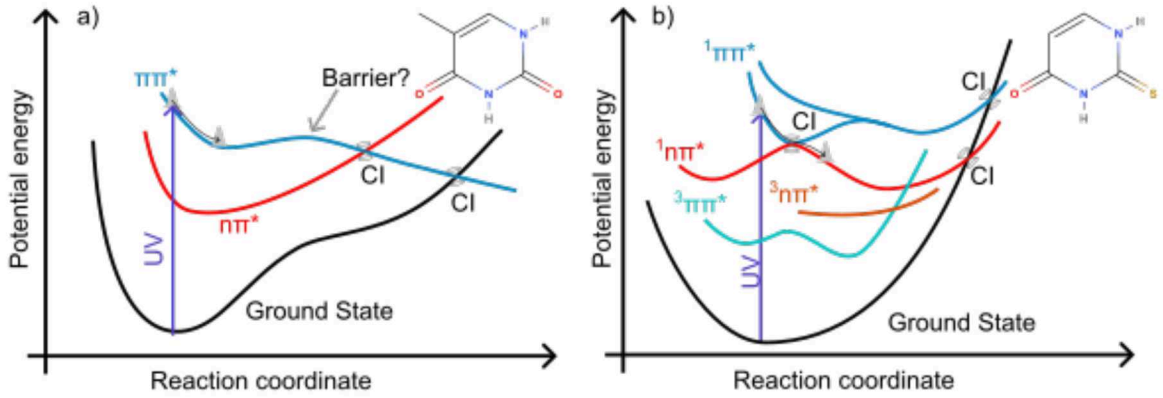

Figure 1: Schemes of the potential energy surfaces of thymine (a) and 2-thiouracil (b). Canonical pyrimidine nucleobases such as thymine show ultrafast relaxation into the ground state after a UV excitation due to conical intersections (CI) among ππ* and nπ* states and the ground state that allow for non-radiative transitions between electronic states. Thionucleobases such as 2-tUra, in contrast, relax efficiently into triplet states because a CI with the ground state is located at a higher energy than the state minimum and a stronger spin-orbit coupling introduced by the sulfur facilitates intersystem crossings close to the minima. Schemes adapted from fig. 1 in ref. [39] and fig. 4 in ref. [14].

For thymine, a sketch of the proposed relaxation pathway is shown in figure 1 a). A strong UV absorption at ca. 265 nm (4.67 eV) prepares an electronic wavepacket in the ππ* state (i.e., an electron is promoted from the π into the unoccupied π* orbital). From the Franck-Condon region the molecule will start to explore the new potential energy landscape and the wavepacket will follow the gradient of the surface converting the excess energy into nuclear motion. Experiments have shown that thymine relaxes efficiently into the ground state within picosecond timescales without fluorescing [40], indicating a relaxation via CIs. Over time, different pathways for that relaxation had been proposed. Some of the calculations suggested a direct ππ* to ground state CI [41,42]. Others proposed an additional, intermediate, 'dark' nπ* state through which the ground state eventually will be repopulated [20,43,44]. In addition, the transition time constants where under question too, as some of the calculations predicted a local ππ* minimum which would increase the relaxation into the ground or nπ* state from below 100 fs without barrier to a few picoseconds [20,41,43].

Experiments on the photoexcited molecule's electronic states show a variety of time constants ranging from femto- to nano- or even microseconds. An early solution phase experiment performed by Reuther et al. using femtosecond absorption spectroscopy found a 1.2 ps lifetime for the lowest excited state [45]. Fluorescence measurements by Gustavsson et al. gave lifetimes of ca. 600 fs [46,47]. Hare et al. measured the lifetimes of thymine using femtosecond transient absorption and infrared spectroscopy and observed lifetimes of 2.8 ps, 30 ps [40] and 0.56 µs [48] which were attributed to a relaxation into the ground state from either the ^{1}ππ*, ^{1}nπ* or the triplet manifold, respectively. TR-PES

experiments in liquids by Buchner et al. yielded lifetimes of 70 fs and 410 fs which were attributed to different conical intersections between the $^1\pi\pi^*$ and the ground state [49]. None of the photoelectron features were attributed to the $n\pi^*$ state in this study. Time-resolved infrared spectra taken by Manna et al. suggested a triplet formation within 4-6 ps depending on the solvent and a very fast $\pi\pi^*$ to ground state relaxation [50]. The fraction of molecules that ended up in the triplet state varied between 4% and 16% depending on the solvent as well. In a very recent study, Miura et al. performed EUV-TRPES on aqueous thymine and observed four time constants for the relaxation [51]. The $\pi\pi^*$ contribution had to be fitted with two lifetimes of 150 fs and 160 fs. An $n\pi^*$ contribution was found with a lifetime of 2.5 ps. Also, a long-lived species with a lifetime larger than 20 ps was observed.

For gas phase experiments comparable values were observed. A study of Kang et al. gave a time constant of 6.4 ps for the relaxation which was attributed to depopulation of the $n\pi^*$ state [52]. Another long decay with >100 ps was assumed to originate from a small number of molecules ending up in triplet states. He et al. and Ligare et al. confirmed a long-lived dark state [52–54]. Following experiments by various groups refined and confirmed three major lifetimes in the thymine relaxation [19,37,51,55–57]. An initial ultrafast relaxation, which ranges between 40 fs and 500 fs, is followed by slightly slower relaxation of up to 10 ps. A third very long decay was observed in the experiments but accurate values could not be given. The assignments of the lifetimes followed mostly the suggestion from Ullrich et al. [19,58]: The $\pi\pi^*$ state decays within a few ten or hundred femtoseconds and populates the $n\pi^*$ state. Within a few picoseconds, this $n\pi^*$ state decays either back into a hot ground state via a conical intersection or undergoes intersystem crossing (ISC) into a ($\pi\pi^*$) triplet state which is supposed to be responsible for the observed nanosecond time constant.

The UV-spectroscopy of photoinduced dynamics of thionated nucleobases differs significantly from their canonical counterparts. The introduction of the sulfur atom lowers the potential energy surfaces in these molecules leading to a significant red-shift in the UV absorption [14,15]. Furthermore, the increased spin-orbit coupling introduced by the sulfur makes inter-system crossings much more likely. Ultrafast ISC times of a few hundred femtoseconds lead to an increased ISC yield close to unity for most of the thionated nucleobases [15]. The triplet lifetimes span from picoseconds to microseconds.

2-thiouracil (2-tUra) is one of the more thoroughly studied thionucleobases both theoretically and experimentally [55,59–65]. A scheme for a potential energy landscape of 2-thiouracil is shown in figure 1 b). Calculations show that the first broad absorption band around 270 nm (4.6 eV) is dominated by transitions into two close lying $\pi\pi^*$ states with slightly different electron localization and similar oscillator strength [66,67]. However, Mai et al. state that excitations of higher lying $\pi\pi^*$ states will relax very quickly into the lowest singlet $^1\pi\pi^*$ state so that their internal dynamics do not play a role in subsequent processes [66]. Interestingly, Mai et al. predict two minima for the lowest $^1\pi\pi^*$ state: one showing strong pyramidalization at the sulfur site ($\pi_S\pi_2^*$), which can also be accessed from higher lying states, and the other showing puckering and pyramidalization at the C_6 atom ($\pi_S\pi_6^*$)

[66]. Both, however, show a CI with the $^1n\pi^*$ state close to their respective minima. According to the calculations, the minimum corresponding to the $\pi_5\pi_6^*$ electronic character might be preferred upon UV excitation [66,68]. Conical intersections between $^1\pi\pi^*$ and the ground state have been predicted but are at higher energies compared to their canonical counterparts [14]. In the vicinity of the $^1n\pi^*$ minimum, the stronger spin-orbit coupling introduced by the sulfur facilitates an intersystem crossing into $^3\pi\pi^*$ triplet states. Again, a CI between $^1n\pi^*$ and ground state is predicted but only reachable via an energy barrier. Intersystem crossing between the ground state and lowest $^3\pi\pi^*$ state is predicted above the $^3\pi\pi^*$ minimum trapping possible population in the triplet manifold.

Experiments, focusing again on probing via valence electrons, support the relaxation pathways proposed by Mai et al. [66,68,69] or Cui and Fang [70] i.e., the relaxation from $^1\pi\pi^*$ via $^1n\pi^*$ into the triplet manifold. Solution-phase transient absorption spectroscopy studies observe two decay constants [62,63]. The first is in the order of a few hundred femtoseconds and is associated with the ISC to the triplet manifold. The response functions in both experiments were not short enough to resolve faster relaxations and, hence, the $^1\pi\pi^* \rightarrow {}^1n\pi^*$ relaxation which is predicted to happen within 100 fs could not be resolved. The second time constant observed is in the order of tens of picoseconds to nanoseconds and is attributed to the triplet lifetime. Gas-phase experiments on 2-tUra were conducted using valence photoelectron spectroscopy [55,61,65] and photoions [59,64]. All of the experiments show three very similar time constants for their observables. The first relaxation happens within less than 100 fs and is attributed to the depopulation of the $^1\pi\pi^*$. The second constant is in the order of a few hundred femtoseconds (200-800 fs) and fits the predicted time-scales for the ISC from the $^1n\pi^*$ to the triplet manifold. The triplet lifetime is measured to be in the order of 100-200 ps through all the experiments.

PROBING ELECTRON AND NUCLEAR DYNAMICS WITH X-RAYS

In this following section, we briefly discuss the basics of the x-ray spectroscopic methods used, as well as their applications on thymine and thiouracil. X-ray probes provide an advantage over optical probing techniques due to element sensitivity and site specificity. Thus, ultrafast x-ray probing allows for a localized view of the molecular dynamics.

Core-level energies differ significantly between elements. For the most important elements in organic compounds S, C, N and O, the 2p and 1s binding energies are separated by over 100 eV starting from around 160 eV for S 2p, 290 eV for C 1s to 410 eV for N 1s and 540 eV for O 1s. The x-ray induced transitions are confined to small electronic core wavefunctions around the respective atoms in molecules, lending the scheme high spatial- or site - fidelity. For instance, probing the sulfur 2p core electrons in 2-tUra via x-ray photoemission gives direct sensitivity to local changes in the vicinity of the sulfur site in 2-tUra. In x-ray photoelectron spectroscopy (XPS, see Fig. 2 a-c), one uses this characteristic binding energy and thus the characteristic kinetic energy E_{kin} of the photoelectron to detect signals originating from the atom of interest. In order to investigate excited state dynamics, a UV

pump x-ray probe scheme can be used. Fig. 2 a) shows an orbital scheme of XPS, with and without a UV excited valence state. The scheme in Fig. 2 b) displays the pump-probe measurement scheme in a multi-electron picture, highlighting the dependence of the binding energy on the nuclear geometry. The UV pulse launches the molecule on the valence-excited PES. Afterwards, the x-ray pulse leads to a core-level cationic state and an outgoing electron with a kinetic energy equal to the difference between the photon energy and the binding energy of the core level.

Site-selectivity is even possible when multiple atoms of the same element are present in the molecule. This is due to so-called chemical shifts, i.e. eV-scale variations in the core-binding energy (and thus XPS kinetic energy) driven by electronegativity variations in the atom's environment [71,72]. The electronegativity of different atoms in the molecule affects the distribution of the valence electrons over the molecule. This, however, impacts the screening of the nuclear charge for core-level electrons and therefore changes their binding energy with respect to the isolated atom. A prime example for this is ethyl-trifluoroacetate ($C_4H_5F_3O_2$), where the four C 1s peaks spread over a 10eV window [71,73]. Similar effects can also be observed in nucleobases and their thionated analogs [38,74,75]. In addition to the chemical shifts observed in molecules when compared to isolated atoms, the binding energy of core levels can be affected by excitations in the electronic state. The changes in electronic density caused by valence excitations affect the screening of nuclear charge that is felt by core electrons. We can exploit this change to follow dynamical processes, by monitoring the changes in core level binding energy as molecular relaxation occurs. Fig. 2 c) shows the redistribution of electric charge on the sulfur atom in 2-tUra that follows photoexcitation. The sensitivity of time-resolved XPS to Excited-State Chemical Shifts (ESCS) and how they relate to the electronic states will be discussed later in this review on the example of 2-tUra.

The concepts of element- and site specificity discussed in the case of XPS also carry on to other x-ray methods, such as to x-ray absorption spectroscopy. Here, a core-level electron is promoted into unoccupied valence orbitals upon absorption of an x-ray photon. As those core-to-valence transitions appear close to the core ionization potential, the method is also called near edge x-ray absorption fine structure (NEXAFS) spectroscopy [76]. Experimentally, NEXAFS spectra can be measured either by detecting the transmitted light or the photoproducts i.e., electrons or ions, as a function of photon energy. The scheme for NEXAFS spectroscopy is shown in Fig2 d-f, again in a single-electron orbital picture (d) and multi-electron PES (e). The transition dipole of the excitation depends significantly on the orbital overlap of the involved core and valence orbital. As the core electrons are strongly confined around individual atoms, transitions will only occur into valence orbitals that have significant electron localization at the respective site. Thus, lone-pair orbitals, as the sulfur *n* orbital indicated in Fig.2f), showing a more atomic character will show a stronger absorption from respective sites than more delocalized valence orbitals such as π orbitals. This can be very helpful for the investigation of relaxation dynamics of molecules where nπ* states play a crucial role.

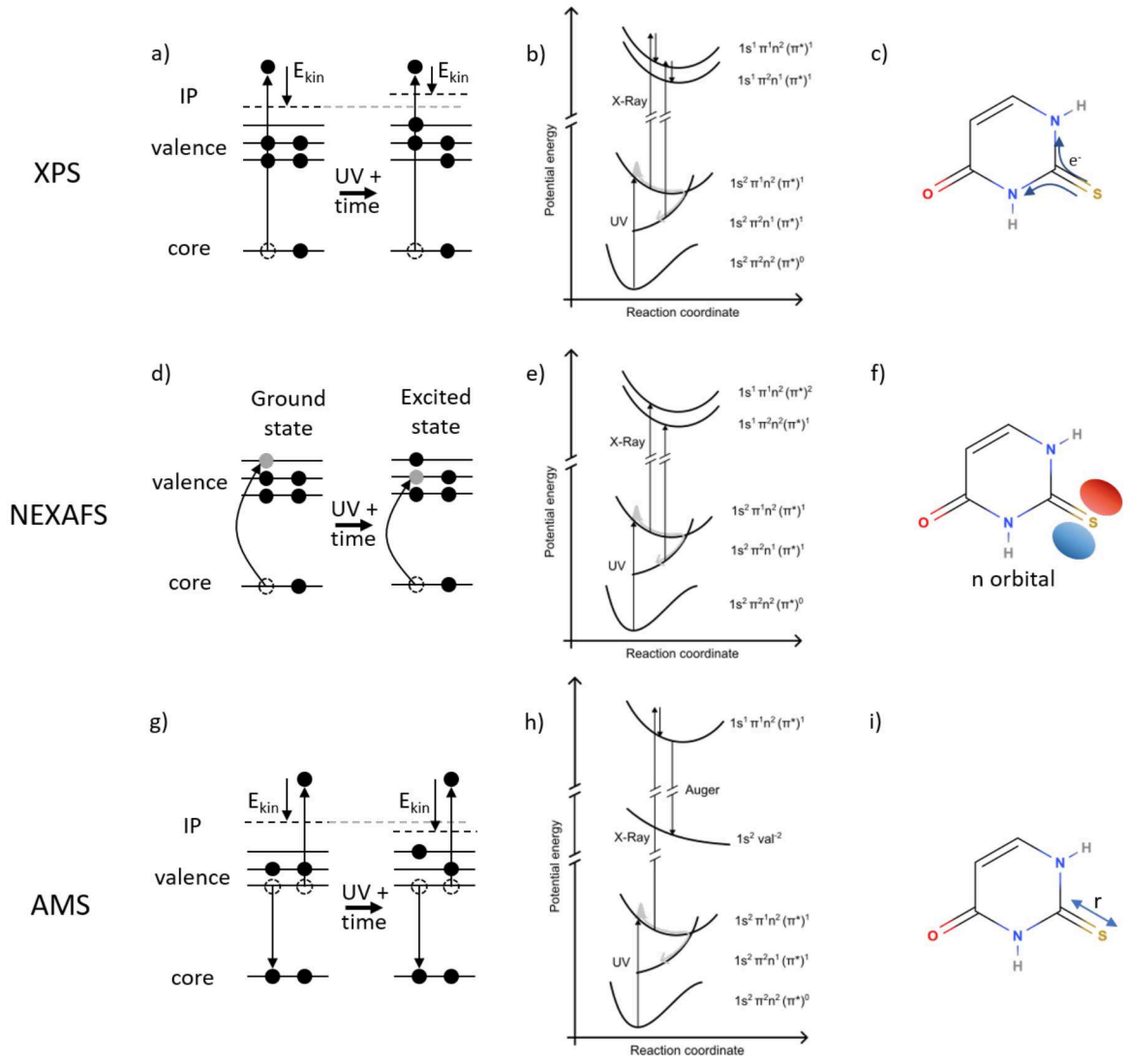

Figure 2: Probing schemes for different x-ray spectroscopic methods addressed in this review and pictograms on how they relate to the molecular problem. The methods covered are x-ray photoelectron spectroscopy (XPS), near edge x-ray absorption fine structure (NEXAFS) and Auger-Meitner spectroscopy (AMS). In the first column, electron balls schemes are shown depicting the x-ray probing mechanism for ground and excited state molecules. The middle column shows sketches of potential energy surfaces. The right column shows the molecules and related observables.

After the creation of a core hole, the molecule is left in a highly excited state. Weaker bound electrons will reoccupy the inner-shell vacancy within tens of femtoseconds. The excess energy can be dissipated in two ways: by emitting a photon or by self-ionization of another valence electron (see Fig.2 g). The first process is known as x-ray fluorescence, and primarily occurs in elements with high nuclear charge ("heavy atoms") as can be deduced from the Einstein coefficients [76]. For lighter atoms such as C, N, O and also S which are main components of organic molecules, the emission of valence electrons via the Auger-Meitner

(AM) effect [77,78] is favored. The energy of the emitted electrons only depends on the binding energies of the involved orbitals i.e., the core level and the valence orbitals. Thus, AM spectroscopy is insensitive to the photon energy and its experimental fluctuations, giving an advantage when compared to the above-mentioned techniques. Attributing spectral features to the plethora of AM transitions, however, requires comparably elaborate theoretical calculations.

The decay of the core hole via AM-transitions involves valence electrons with a high localization at the core-hole site. Thus, AM spectroscopy is sensitive to structural changes in the vicinity of the atom. Since a major part of the total energy of the (di-)cationic final states is stored in the Coulomb repulsion between the positively charged neighboring atoms, the bond distance affects the resulting AM electron kinetic energy. This sensitivity, however, only allows for qualitative statements on geometric changes. For more quantitative results on the nuclear configuration, time-resolved diffraction experiments are better suited to study the geometry (changes). Those experiments have been accomplished with femtosecond time resolution using hard x-ray pulses [79–83] and also ultrashort electron pulses [84–87].

Experimental setup

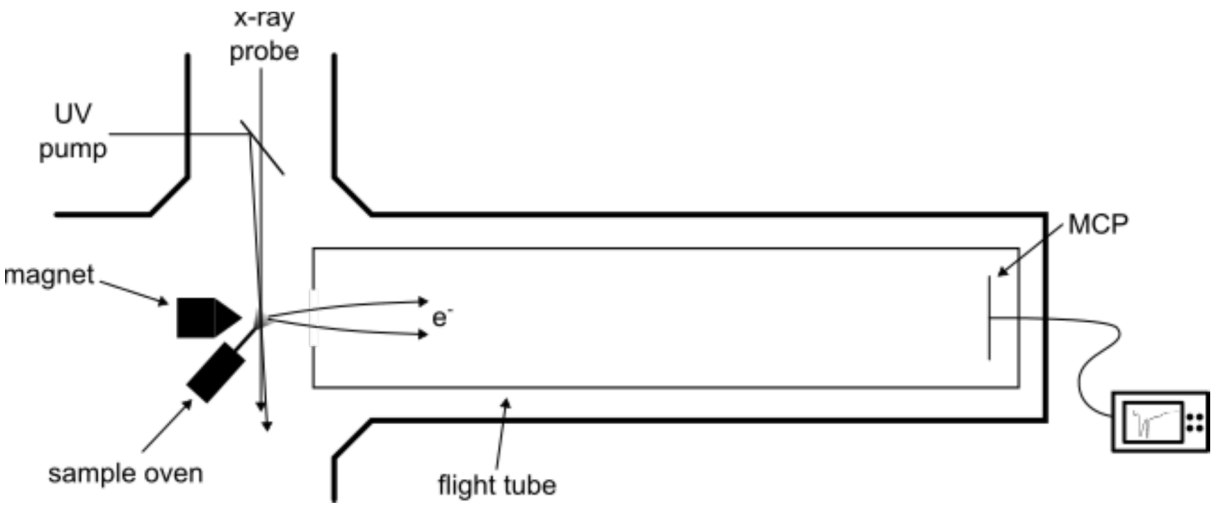

Figure 3: Sketch of the experimental setup. A UV-pump x-ray probe scheme was used in all experiments. Photo- and Auger-Meitner electrons were collected using a magnetic bottle time-of-flight spectrometer.

The experiments that will be discussed in the following sections were conducted at different free-electron laser facilities, namely the linac coherent light source (LCLS) at SLAC National Accelerator Laboratory, USA [22], and the FLASH free electron laser at DESY in Hamburg, Germany [21,88,89]. Free-electron lasers are powerful tools for the measurements as they provide short (femtosecond) and intense light pulses in a broad spectral region reaching from the THz to hard x-ray domain.

The experimental setup for time-resolved XPS, NEXAFS and AM are identical and

determined by the fact that the sample consists of isolated molecules. In the following we will briefly describe the experimental scheme. Details of the apparatus at LCLS can be found in refs. [39,90] and for FLASH in ref. [91]. A sketch is shown in figure 3. The molecules which are solid at room temperature are brought into gas phase via an in-vacuum oven system described in ref. [39]. With this system, the molecules can be heated up to ca. 150°C and the vapor is directed to the interaction region with a small capillary at the end of the oven.
The molecules are excited with a UV pump pulse with a wavelength around 270 nm and sub-100 fs pulse duration. The pulse energy is usually chosen in a way such that only a fraction of the molecules are excited in order to avoid nonlinear effects. An x-ray pulse provided by the FEL is tuned to core-excite or ionize the respective atoms probes the molecule. Photo- and Auger-Meitner electrons are collected and their kinetic energy is determined using a magnetic bottle electron time-of-flight spectrometer (MBES). The MBES allows for a high collection efficiency of almost 4π, due to its inhomogeneous and guiding magnetic field [92]. This large collection efficiency is favorable for dilute gas phase spectroscopy.

Time-resolved NEXAFS spectroscopy

We now present time-resolved NEXAFS spectra of thymine at the oxygen edge. The experiment delivers information which is complementary to the time resolved absorption and valence photoelectron spectroscopy. The static x-ray absorption spectra of isolated thymine at the oxygen edge observed in an experiment at LCLS (figure 4 a), black line) [93] agree with synchrotron measurements [74]. Two absorption peaks are observable at 531.5eV and 532.5eV photon energy which can be attributed to transitions from the oxygen 1s into linear combinations of π* orbitals which conserve the high localization of electrons at the respective oxygen atom.
We now concentrate on the effect of molecular UV excitation on the NEXAFS spectra [93]. The result for 2ps delay between UV pump and x-ray probe pulse is shown in figure 4 a) (green line). The main observation is the appearance of a new feature at around 526.5 eV. In addition, a very subtle bleach of the original 1s-π* band can be observed around 531.5 eV which is due to a depopulation of the ground state. However, it is almost entirely compensated by a redshift of the K edge ionization feature in the excited state [93] and, hence, only barely visible in fig. 4a). The new appearing feature, which is located one UV photon quantum below the main resonance, represents a new absorption channel due to the UV-induced rearrangement of valence electrons. As the UV induces a ππ* transition, a new 1s-π absorption channel opens. In addition, after the ππ*-nπ* relaxation, which is the matter of this investigation, an 1s-n transition will show up in the absorption spectrum. The transition from a core-orbital to a lone pair orbital at the same atom is very strong, stronger than core-valence transitions to delocalized orbitals. Intuitively one would expect that the oxygen 1s-n transition dominates the UV-induced NEXAFS feature, and this was also confirmed by a transition-strength calculation in [93]. This strong atomic absorption feature has also been used in a liquid jet experiment of water radiolysis [94].

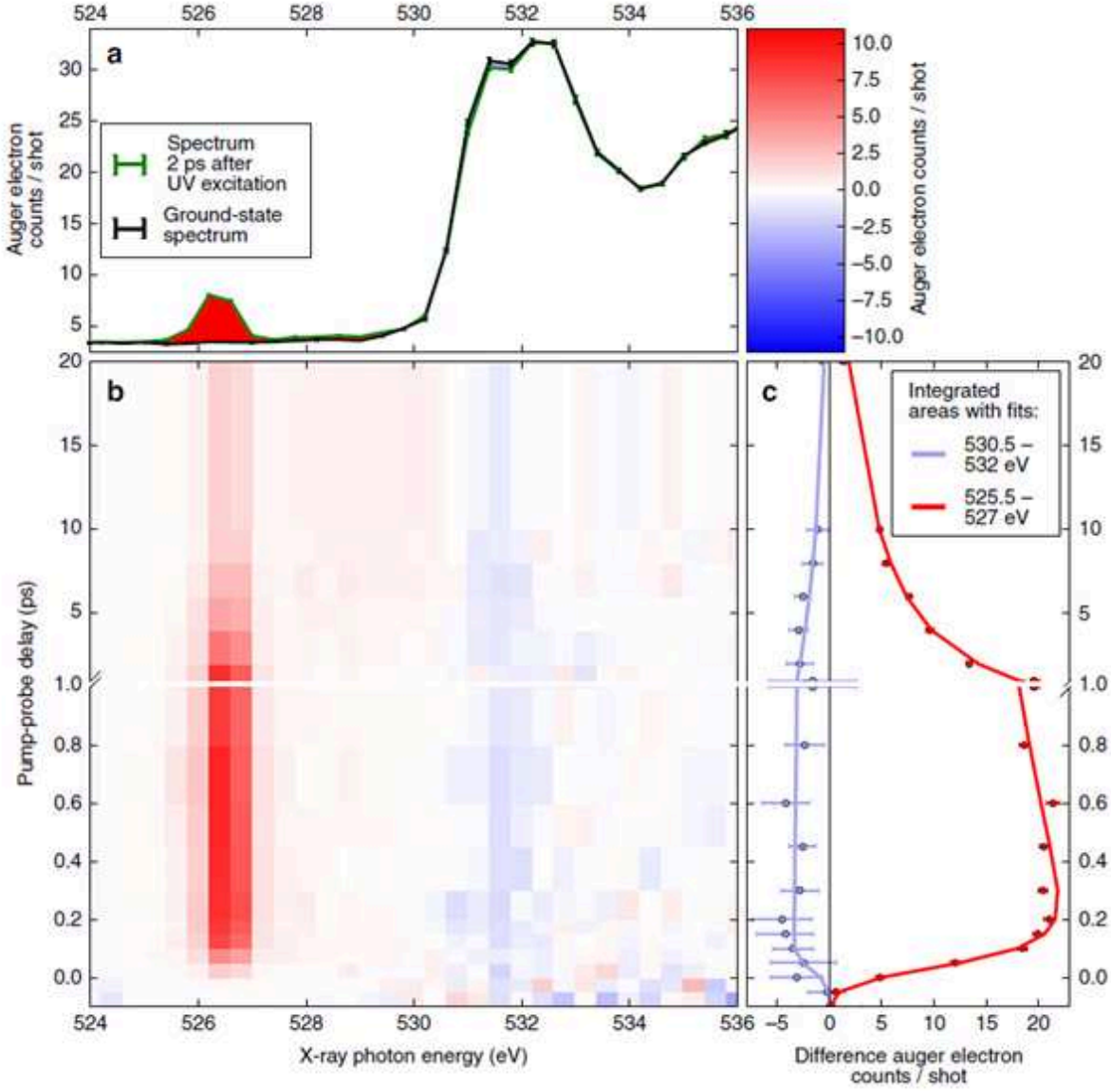

Figure 4: a) Ground and excited-state NEXAFS spectrum of thymine. The red bump indicates the appearance of a new strong feature in the UV excited spectrum. b) Delay-dependent false-color map of NEXAFS difference spectra. c) Integrated regions of interest in the false-color map. A slight shift of the rising edge can be observed between bleach and gain features. The figure was taken from Fig. 2 in Ref. [93] without changes and reused under a Creative Commons Attribution 4.0 International (CC BY 4.0) License.

The two-dimensional false color plot in figure 4 b) shows the time-resolved bleach at the 1s-π* resonance (531 eV, blue) and rise of the 1s-n resonance (526.5 eV, red). This reveals the dynamics of the ππ*-nπ* relaxation. The bleach at zero delay of pump and probe indicates the UV induced ππ* excitation. The 1s-n absorption signal, reflecting the nπ* population, occurs with a delay of ca. 60fs. We therefore attribute a time constant of 60 fs to the ππ*-nπ* relaxation in agreement with the first attributions [19] but in strong contrast to the

picosecond constant predicted later [20,43,95]. The 60fs time constant for the ππ*-nπ* relaxation demonstrates a very direct path for access to an efficient internal conversion.
Transient x-ray absorption spectroscopy is an important technique in the hard x-ray domain and it is mainly used in the context of metal-containing molecules in liquid environments [96,97]. In gas phase and the soft x-ray domain, several ultrafast experiments using inherently broadband high harmonic generation sources have been performed. The investigate for instance strong field ionization dynamics and UV excited ring-opening reactions [98–101].

Time-resolved x-ray photoelectron spectroscopy

The electronic relaxation of molecules through different electronic states after excitation is often accompanied by significant movement of valence charge around the molecule. This relocation of electric charge affects the screening of nuclear charge for strongly localized electrons and, hence, will impact their binding energy. In the case of 2-thiouracil, the two highest occupied molecular orbitals, the π and the n orbital, show significant localization at the sulfur atom. The unoccupied π* orbital - which is the electron's destination for the first optically excitable transition in the molecule- shows, in contrast, a strong delocalization over the pyrimidine ring. An excitation from π to π* will, thus, shift electron charge from the sulfur to the ring. This is shown in the charge difference maps in Fig. 5 a). The red color indicates a more positive charge with respect to the molecular ground state and blue more negative charge. The sulfur indeed loses valence charge while the neighboring carbon atom seems to receive most of it. With the decrease of screening at the sulfur it can be expected that core-localized electrons at the sulfur, i.e. 1s, 2s and, 2p, will increase their binding energy due to a higher Coulomb force. Vice versa, the C 1s electron would be expected to reduce their binding energy due to an increased screening.
We have measured the time-resolved photoelectron spectra at the sulfur site of 2-tUra at FLASH free electron laser [102]. The fig. 5 b) shows the static (blue) and pre-excited (orange) spectrum for the S 2p photoelectrons. Due to the relatively large bandwidth of the FEL, the spin orbit splitting of the photoline cannot be resolved. Synchrotron data (shown in black) shows the fine structure in the electron spectrum. The photoline is accompanied by a small satellite feature at lower kinetic energies originating from shake-up processes during the ionization. The UV excitation of the molecule alters the shape of the spectrum. The main photoline bleaches and new signal rises at lower kinetic energies. The shift of the excited state signal amounts to ca. -3 eV. This indicates an increase of the binding energy for the S 2p electrons which agrees with the above made prediction.
The observed shift is an immediate response after the excitation and lasts for at least 100ps which agrees with previous results on the lifetime of the triplet states. Figure 5 c) shows the excited state signal for small delays between pump and probe pulse as a false color map. Following the contour lines, a change of the shape of the feature can be observed within the first picosecond of the relaxation that follows an oscillatory behavior. The band broadens

towards lower kinetic energies and contracts again over a course of ca. 250 fs. Such changes

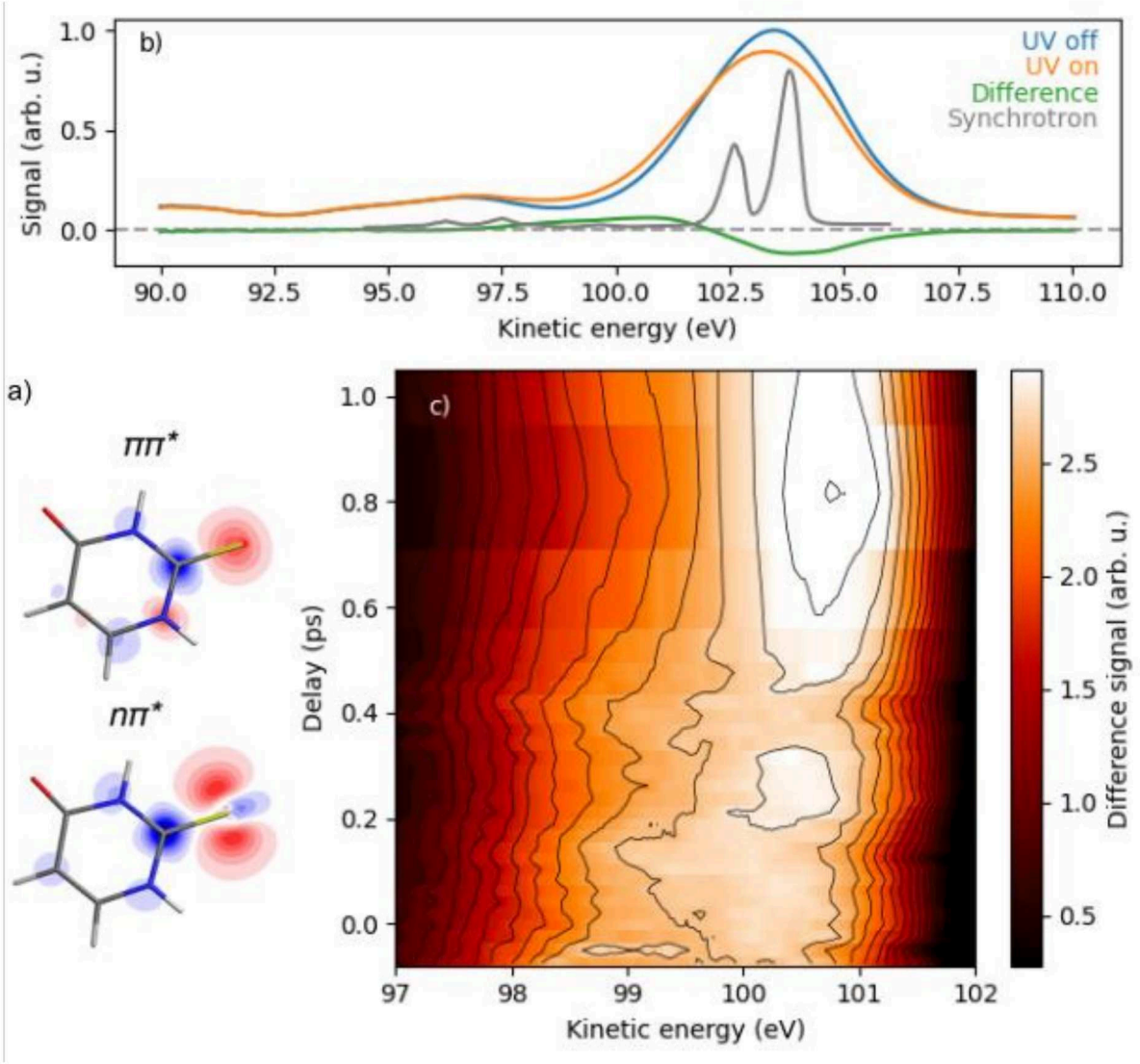

Figure 5: a) Computed charge difference maps for $^1\pi\pi^*$ and $^1n\pi^*$ states. Red indicates more positive charge compared to ground state, blue indicates more negative charge. b) Photoelectron spectra of 2-tUra for the ground ("UV-off") and excited state ("UV-on") at 500fs delay as well the difference spectrum. A static spectrum measured at the PLEIADES beamline of the synchrotron SOLEIL (grey) is included for comparison. c) Delay-dependent false-color map of the positive lobe of the difference spectrum.

in kinetic energy can indicate changes in the electronic character of the excited state during the relaxation. Here, it can be an indication of coherent charge flow between ππ* and nπ* states as a hole in the lone-pair orbital would decrease the screening at the sulfur further. Previous calculation by Mai et al. also show oscillatory behavior in the population of the nπ* states [68,69] which match the experimental oscillation strengthening the assumption of coherent charge flow due to changes in the electronic state.

Coupled-cluster calculations, which we performed for the study, confirm the strong

correlation between local valence charge, core-level binding energy and electronic states. Both singlet and triplet nπ* states show the highest partial charge at the sulfur and also the highest shift in binding energy while ππ* states give rise to less but still significant redshifts. The calculations also suggest that geometrical changes during the relaxation play little to no role.

Studies on time-resolved XPS on small molecules are still rather limited but other recent experiments show the possibilities the method offers. In 2018, Leitner et al. [103] and Braußе et al. [104] published the first studies where ultrashort x-ray pulses from FLASH were used to investigate dissociation dynamics of small molecules in the gas phase. Braußе et al. studied the photodissociation of CH3I using velocity map imaging of electrons and ions [104]. They were able to identify a chemical shift in the electron spectra that corresponded to the formation of atomic iodine with a rise time of ca. 20fs coinciding with the temporal resolution of their experiment. Leitner et al. studied the photodissociation of iron carbonyls using a magnetic-bottle time-of-flight spectrometer [103]. The chemical shifts observed in $Fe(CO)_3$, $Fe(CO)_4$ and $Fe(CO)_5$ gave insight into the bond changes between the different complexes.

More recent studies have further pushed the capabilities of TRXPS. Allum et al. studied the photodissociation of 1-iodo-2-methylbutane also at FLASH [105]. In the experiment, the group exploited the dual-sided velocity map imaging setup of the CAMP endstation at FLASH1 to test a electron-ion partial covariance imaging scheme for photoelectron spectroscopy. Chemical shifts observed in the I 4d photoline could again be attributed to the formation of atomic iodine. Faccialà et al. used circularly polarized x-ray pulses from FERMI to investigate the photoexcited Rydberg states of fenchone by a combination of TRXPS and time-resolved photoelectron circular dichroism (TR-PECD) [106]. The chemical shift observed in the x-ray photoelectron spectra could be attributed to charge relocation as the highest occupied molecular, which is depopulated upon excitation, is a lone pair orbital localized at the C_1, C_2 and C_3 atoms. The combination with the PECD, however, appears challenging due to the low signal-to-noise ratio during the experiment. Nonetheless, the UV-induced chemical shift isolated the C_2/C_3 contribution in the PECD whose dynamics could thus be studied and rationalized. Gabalski et al. recently revisited the photodissociation dynamics of CS_2 using TRXPS at FLASH [107]. They show that the experimentally observed chemical shift upon UV excitation can be attributed to the formation of the photofragments CS and S as their binding energy drastically differs from CS_2. In addition, they show that TRXPS is also sensitive to the vibronic state of the fragments. Though most of the studies mentioned here face different problems such as limited signal-to-noise or a lack of energy or temporal resolution, they show the capabilities of TRXPS for studying ultrafast relaxation processes and with future improvements of FELs these limitations might be overcome.

Time-resolved Auger-Meitner spectroscopy

We have investigated both Thy and 2-tUra by means of AM spectroscopy [39,108,109]. The measurements on Thy were performed at LCLS, those for 2-tUra again at FLASH2. Some results for the time-resolved non-resonant AM spectroscopy of Thy from Ref [39] are shown

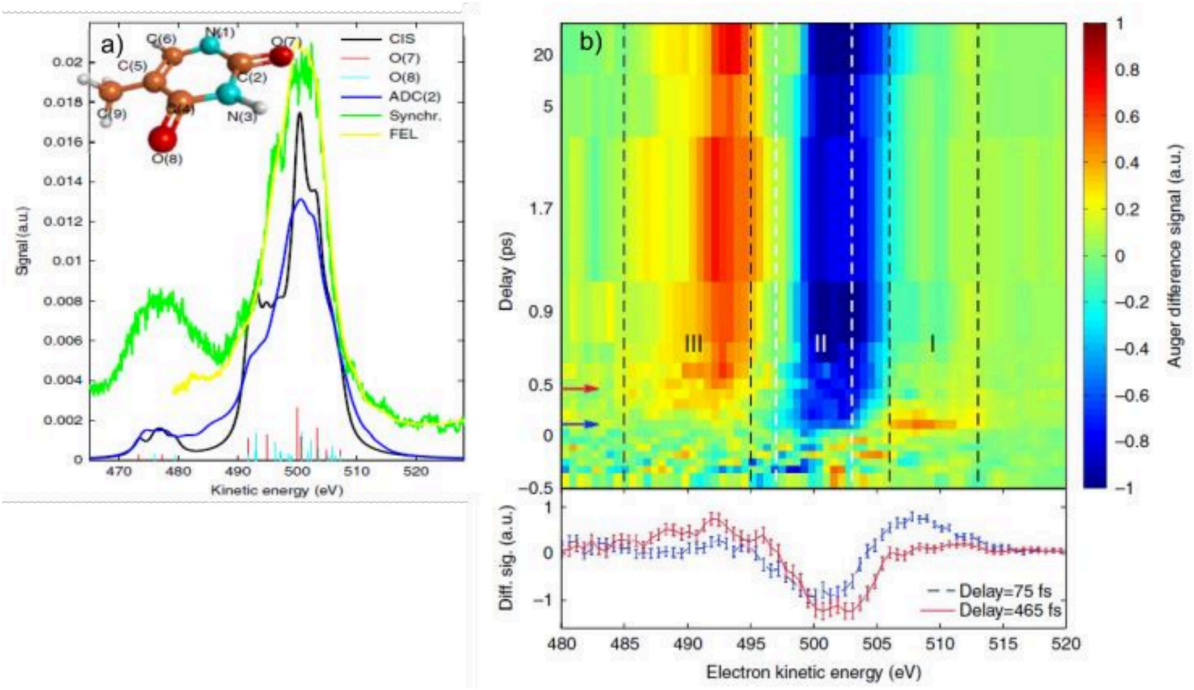

Figure 6: a) Static Auger-Meitner spectra of thymine. Synchrotron (green) and FEL (yellow) measurements of the ground-state spectrum are shown together with ADC (blue) and CK-CIS calculations (black). The stick spectra (red and cyan) come from the CK-CIS calculations and indicate transitions from the respective oxygen atoms which produce similar Auger-Meitner spectra to those shown. b) The top panel shows the delay-dependent false-color map of the difference between ground-state and UV-excited AM spectra of thymine. The bottom panel shows two lineouts from the false-color map which are indicated by the arrows in the plot above. Material taken from figs. 2 and 3 in ref. [39] without changes.

in fig. 6. To trigger the AM decay, the O 1s electrons were ionized. The ground-state spectrum is shown in fig 6 a). Two broad bands can be observed between 470eV and 520eV kinetic energy. Upon UV excitation the FEL measurements show a shift of the higher energetic band (see b). Initially, the Auger-Meitner spectrum shifts towards higher energies but it decays fast in the order of 100fs and a shift towards lower energies is observed. The quick decay of the first feature already suggests that there might not be a significant energy barrier in the $\pi\pi^*$ state trapping population.

The initial shift towards higher energies can be explained based on a nuclear relaxation. The created dicationic state is highly repulsive due to unscreened nuclear charge around the C-O bond. A higher Coulomb repulsion, however, leads to a bond elongation which in consequence leads to a lower energy of the dicationic final states. The spectrum shifts towards higher kinetic energies. The quick relaxation of these features and the shift towards

lower energies with respect to the ground state, however, contrast a further nuclear relaxation and suggest an electronic relaxation. In combination with dynamics calculations, the results again towards an ultrafast relaxation channel into singlet nπ* state.

Similar experiments were performed at FLASH with 2-tUra [108]. Here, the sulfur 2p edge was probed and the Auger band was recorded. Again, a fast shift towards higher kinetic energies can be observed upon UV excitation. This shift can be also attributed to a nuclear relaxation. The reduction of nuclear charge screening upon ionization of the S 2p electrons favors a C-S bond elongation to minimize the energy of the cationic states. An elongation of the C-S bond upon excitation was predicted by previous theoretical studies [66,68]. Further dynamics of the Auger band, however, cannot be explained by a pure nuclear relaxation and must be the results of electronic relaxation. Simulating Auger-Meitner spectra in detail is relatively elaborate, and this is the reason that very little studies use this as an observable. For low-lying dicationic states however this restriction is somewhat eased.

Resonant AM decay can be used to derive the x-ray absorption spectra of molecules as resulting Auger electrons lead to an enhancement in the electron yield and, thus, can indicate resonant excitation channels. The absorption spectra in [93] were derived that way. The underlying resonant AM decays were studied in [109], and two interfering de-excitation channels are observed. One of these de-activation channels is the population of a ππ* triplet state which has been also proposed in a previous VUV study [57].

DEVELOPMENT OF THE FIELD

Several developments are currently occurring using ultrafast x-rays as probe methods. First, new, higher repetition rate FEL sources are available with the European XFEL, at an effective repetition rate of 27 kHz, and LCLS II, at a projected repetition rate of 1 MHz. The high repetition rate allows for using charge particle coincidence methods, such as COLTRIMS reaction microscopy [110,111] for time-resolved molecular spectroscopy, and first examples from these sources on molecules in the ground state show the power of Coulomb explosion imaging for retrieving the molecular geometry [30]. In addition, the signal-to-noise in any of the spectroscopic schemes presented above will increase, allowing for investigation of dilute samples and also of samples in a liquid phase environment, where an additional background from absorption of the jet poses difficulties at some x-ray edges at current repetition rates.

A further promising development in the FEL community is the scaling of external seeding to higher repetition rates. Currently, almost all free-electron lasers rely on self-amplified spontaneous emission (SASE), meaning they deliver a noisy spectral and temporal structure that changes with every shot. The FERMI free electron laser [23] presents a famous exception, as it is externally seeded by a UV laser and operates at harmonics of this radiation. This results in high longitudinal coherence and excellent spectral stability. Scaling the seeding scheme from around 100 Hz at FERMI to higher repetition rates will allow to explore many more methodologies, such as resonant inelastic x-ray scattering [112], ion trap spectroscopy and again coincidence methods. At the FLASH free-electron laser, seeded

operation up to 5 kHz effective repetition rate is planned [113]. The increased spectral control with more coherent x-ray laser sources will also result in the realization of nonlinear probe schemes [114–116] building experimental success with lasing and Raman emission with SASE sources [117,118].

With regard to the development of sample sources, different techniques have been developed in the past to bring large molecules into the gas-phase, for example matrix-assisted laser desorption/ionization [119] or electrospray ionization [120]. They find application so far mostly limited to mass spectrometry. However, there is ongoing work in improving those techniques with respect to sample density, stability and their application in electron or coincidence measurements [121,122]. Laser-induced acoustic desorption was already used in femtosecond spectroscopy with laboratory laser sources [123,124] and could be an option at free-electron lasers. There is also ongoing work in purifying molecular sample beams and selecting individual conformers and quantum states [125–127].

CONCLUSIONS

The advent of short-wavelength FELs in the last decade started the investigation of light-induced, ultrafast molecular dynamics using femtosecond x-ray pulses. Utilizing the element- and site-selectivity of x-rays allows to disentangle electronic and nuclear degrees of freedom during the relaxation and test proposed relaxation pathways more directly. In this review we have discussed the applications of different x-ray spectroscopy methods for investigating the relaxation dynamics of molecules based on our research on the well-studied nucleobase thymine and the thionucleobase 2-thiouracil.

We showed that the ambiguity in the proposed relaxation pathway for the molecule thymine could be solved with the help of x-ray absorption spectroscopy [93]. By directly accessing resonant transitions between the oxygen 1s core and the half empty n-valence orbitals, the optically dark $n\pi^*$ could be observed as a UV-induced feature in the absorption spectrum. In combination with an observed 60 fs delay in its appearance, this technique allowed to unambiguously point towards a sub-100 fs internal conversion from the $\pi\pi^*$ into the $n\pi^*$ state without delays by a previously suggested energy barrier.

We studied the UV-induced excited-state chemical shifts in the x-ray photoelectron spectra of 2-thiouracil. We discovered the connection between shift and valence charge flow over the molecule upon UV excitation [102]. This agrees with the classical model of chemical shifts, where the binding energy of core-level electrons is strongly dependent on the local valence electronic charge. We succeed in observing the electronic changes due to internal conversion and intersystem crossing that lead to a redistribution of charge over the molecule. Probing the binding energies of core electrons at different sites and elements inside the molecules will allow to track charge movement completely and will thus create an electronic molecular movie.

Time-resolved Auger-Meitner spectroscopy shows sensitivity to geometrical changes in the vicinity of the core-hole. Both thymine and 2-thiouracil show an initial shift in the Auger-Meitner electron energy towards higher kinetic energies at the O 1s and S 2p edges, respectively [39,108]. From electrostatic considerations, this can be attributed to an initial bond elongation between carbon and the respective heteroatom. However, further relaxation dynamics cannot be attributed to geometrical changes, more expensive theoretical models are needed to capture the electronic relaxation that drives AM spectral shifts after the initial bond elongation. In future, time-resolved Coulomb-explosion imaging and ultrafast x-ray or electron diffraction, will allow to follow the nuclear geometry changes with much higher level of detail. Together with the high-fidelity data on electronic dynamics, this will allow for the reconstruction of the complete electronic and nuclear geometry changes in molecular excited-state dynamics.

In the future, the ongoing development of FELs in terms of repetition rate and seeding will enable a wide range of spectroscopic techniques for molecular samples to study both nuclear and electronic degrees of freedom in a time-resolved manner. Ongoing development on sources for more complex samples will also allow for the investigation of much larger biological systems than presented in this review.

REFERENCES

1. Kneuttinger, A.C., Kashiwazaki, G., Prill, S., Heil, K., Müller, M., and Carell, T. (2014) Formation and Direct Repair of UV-induced Dimeric DNA Pyrimidine Lesions. *Photochem. Photobiol.*, **90** (1), 1–14.
2. Crespo-Hernández, C.E., Cohen, B., Hare, P.M., and Kohler, B. (2004) Ultrafast Excited-State Dynamics in Nucleic Acids. *Chem. Rev.*, **104** (4), 1977–2020.
3. Barbatti, M., Borin, A.C., and Ullrich, S. (eds.) (2015) *Nucleobases in the gas phase and in solvents*, Springer, Cham.
4. Schreier, W.J., Schrader, T.E., Koller, F.O., Gilch, P., Crespo-Hernandez, C.E., Swaminathan, V.N., Carell, T., Zinth, W., and Kohler, B. (2007) Thymine Dimerization in DNA Is an Ultrafast Photoreaction. *Science*, **315** (5812), 625–629.
5. Astwood, E.B. (1943) Treatment of hyperthyriodism with thiourea and thiouracil. *J. Am. Med. Assoc.*, **122** (2), 78.
6. Astwood, E.B., Vanderlaan, W.P., Hospital, B., and Hospital, P.D. (1945) Thiouracil Derivatives of Greater Activity for the Treatment of Hyperthyroidism. (March 2015), 424–430.
7. Swann, P.F., Waters, T.R., Moulton, D.C., Xu, Y.-Z., Zheng, Q., Edwards, M., and Mace, R. (1996) Role of Postreplicative DNA Mismatch Repair in the Cytotoxic Action of Thioguanine. *Science*, **273** (5278), 1109–1111.
8. Palumbo, A., and D'Ischia, M. (2001) Thiouracil Antithyroid Drugs as a New Class of Neuronal Nitric Oxide Synthase Inhibitors. *Biochem. Biophys. Res. Commun.*, **282** (3), 793–797.

9. Ortiz-Rodríguez, L.A., and Crespo-Hernández, C.E. (2020) Thionated organic compounds as emerging heavy-atom-free photodynamic therapy agents. *Chem. Sci.*, **11** (41), 11113–11123.
10. Zhang, S., Blain, J.C., Zielinska, D., Gryaznov, S.M., and Szostak, J.W. (2013) Fast and accurate nonenzymatic copying of an RNA-like synthetic genetic polymer. *Proc. Natl. Acad. Sci.*, **110** (44), 17732–17737.
11. Szostak, J.W. (2012) The eightfold path to non-enzymatic RNA replication. *J. Syst. Chem.*, **3** (1), 2.
12. Rios, A.C., and Tor, Y. (2013) On the Origin of the Canonical Nucleobases: An Assessment of Selection Pressures across Chemical and Early Biological Evolution. *Isr. J. Chem.*, **53** (6–7), 469–483.
13. Middleton, C.T., de La Harpe, K., Su, C., Law, Y.K., Crespo-Hernández, C.E., and Kohler, B. (2009) DNA Excited-State Dynamics: From Single Bases to the Double Helix. *Annu. Rev. Phys. Chem.*, **60** (1), 217–239.
14. Arslancan, S., Martínez-Fernández, L., and Corral, I. (2017) Photophysics and Photochemistry of Canonical Nucleobases' Thioanalogs: From Quantum Mechanical Studies to Time Resolved Experiments. *Molecules*, **22** (6), 998.
15. Ashwood, B., Pollum, M., and Crespo-Hernández, C.E. (2019) Photochemical and Photodynamical Properties of Sulfur-Substituted Nucleic Acid Bases,. *Photochem. Photobiol.*, **95** (1), 33–58.
16. Improta, R., Santoro, F., and Blancafort, L. (2016) Quantum Mechanical Studies on the Photophysics and the Photochemistry of Nucleic Acids and Nucleobases. *Chem. Rev.*, **116** (6), 3540–3593.
17. Yarkony, D.R. (1996) Diabolical conical intersections. *Rev. Mod. Phys.*, **68** (4), 985–1013.
18. Domcke, W., Yarkony, D., and Köppel, H. (eds.) (2004) *Conical intersections electronic structure, dynamics & spectroscopy*, World Scientific, River Edge, N.J.; London.
19. Ullrich, S., Schultz, T., Zgierski, M.Z., and Stolow, A. (2004) Electronic relaxation dynamics in DNA and RNA bases studied by time-resolved photoelectron spectroscopy. *Phys. Chem. Chem. Phys.*, **6** (10), 2796.
20. Hudock, H.R., Levine, B.G., Thompson, A.L., Satzger, H., Townsend, D., Gador, N., Ullrich, S., Stolow, A., and Martínez, T.J. (2007) Ab Initio Molecular Dynamics and Time-Resolved Photoelectron Spectroscopy of Electronically Excited Uracil and Thymine. *J. Phys. Chem. A*, **111** (34), 8500–8508.
21. Ackermann, W., Asova, G., Ayvazyan, V., Azima, A., Baboi, N., Bähr, J., Balandin, V., Beutner, B., Brandt, A., Bolzmann, A., Brinkmann, R., Brovko, O.I., Castellano, M., Castro, P., Catani, L., Chiadroni, E., Choroba, S., Cianchi, A., Costello, J.T., Cubaynes, D., Dardis, J., Decking, W., Delsim-Hashemi, H., Delserieys, A., Di Pirro, G., Dohlus, M., Düsterer, S., Eckhardt, A., Edwards, H.T., Faatz, B., Feldhaus, J., Flöttmann, K., Frisch, J., Fröhlich, L., Garvey, T., Gensch, U., Gerth, Ch., Görler, M., Golubeva, N., Grabosch, H.-J., Grecki, M., Grimm, O., Hacker, K., Hahn, U., Han, J.H., Honkavaara, K., Hott, T., Hüning, M.,

Ivanisenko, Y., Jaeschke, E., Jalmuzna, W., Jezynski, T., Kammering, R., Katalev, V., Kavanagh, K., Kennedy, E.T., Khodyachykh, S., Klose, K., Kocharyan, V., Körfer, M., Kollewe, M., Koprek, W., Korepanov, S., Kostin, D., Krassilnikov, M., Kube, G., Kuhlmann, M., Lewis, C.L.S., Lilje, L., Limberg, T., Lipka, D., Löhl, F., Luna, H., Luong, M., Martins, M., Meyer, M., Michelato, P., Miltchev, V., Möller, W.D., Monaco, L., Müller, W.F.O., Napieralski, O., Napoly, O., Nicolosi, P., Nölle, D., Nuñez, T., Oppelt, A., Pagani, C., Paparella, R., Pchalek, N., Pedregosa-Gutierrez, J., Petersen, B., Petrosyan, B., Petrosyan, G., Petrosyan, L., Pflüger, J., Plönjes, E., Poletto, L., Pozniak, K., Prat, E., Proch, D., Pucyk, P., Radcliffe, P., Redlin, H., Rehlich, K., Richter, M., Roehrs, M., Roensch, J., Romaniuk, R., Ross, M., Rossbach, J., Rybnikov, V., Sachwitz, M., Saldin, E.L., Sandner, W., Schlarb, H., Schmidt, B., Schmitz, M., Schmüser, P., Schneider, J.R., Schneidmiller, E.A., Schnepp, S., Schreiber, S., Seidel, M., Sertore, D., Shabunov, A.V., Simon, C., Simrock, S., Sombrowski, E., Sorokin, A.A., Spanknebel, P., Spesyvtsev, R., Staykov, L., Steffen, B., Stephan, F., Stulle, F., Thom, H., Tiedtke, K., Tischer, M., Toleikis, S., Treusch, R., Trines, D., Tsakov, I., Vogel, E., Weiland, T., Weise, H., Wellhöfer, M., Wendt, M., Will, I., Winter, A., Wittenburg, K., Wurth, W., Yeates, P., Yurkov, M.V., Zagorodnov, I., and Zapfe, K. (2007) Operation of a free-electron laser from the extreme ultraviolet to the water window. *Nat. Photonics*, **1** (6), 336–342.

22. Emma, P., Akre, R., Arthur, J., Bionta, R., Bostedt, C., Bozek, J., Brachmann, A., Bucksbaum, P., Coffee, R., Decker, F.-J., Ding, Y., Dowell, D., Edstrom, S., Fisher, A., Frisch, J., Gilevich, S., Hastings, J., Hays, G., Hering, P., Huang, Z., Iverson, R., Loos, H., Messerschmidt, M., Miahnahri, A., Moeller, S., Nuhn, H.-D., Pile, G., Ratner, D., Rzepiela, J., Schultz, D., Smith, T., Stefan, P., Tompkins, H., Turner, J., Welch, J., White, W., Wu, J., Yocky, G., and Galayda, J. (2010) First lasing and operation of an angstrom-wavelength free-electron laser. *Nat. Photonics*, **4** (9), 641–647.

23. Allaria, E., Appio, R., Badano, L., Barletta, W.A., Bassanese, S., Biedron, S.G., Borga, A., Busetto, E., Castronovo, D., Cinquegrana, P., Cleva, S., Cocco, D., Cornacchia, M., Craievich, P., Cudin, I., D'Auria, G., Dal Forno, M., Danailov, M.B., De Monte, R., De Ninno, G., Delgiusto, P., Demidovich, A., Di Mitri, S., Diviacco, B., Fabris, A., Fabris, R., Fawley, W., Ferianis, M., Ferrari, E., Ferry, S., Froehlich, L., Furlan, P., Gaio, G., Gelmetti, F., Giannessi, L., Giannini, M., Gobessi, R., Ivanov, R., Karantzoulis, E., Lonza, M., Lutman, A., Mahieu, B., Milloch, M., Milton, S.V., Musardo, M., Nikolov, I., Noe, S., Parmigiani, F., Penco, G., Petronio, M., Pivetta, L., Predonzani, M., Rossi, F., Rumiz, L., Salom, A., Scafuri, C., Serpico, C., Sigalotti, P., Spampinati, S., Spezzani, C., Svandrlik, M., Svetina, C., Tazzari, S., Trovo, M., Umer, R., Vascotto, A., Veronese, M., Visintini, R., Zaccaria, M., Zangrando, D., and Zangrando, M. (2012) Highly coherent and stable pulses from the FERMI seeded free-electron laser in the extreme ultraviolet. *Nat. Photonics*, **6** (10), 699–704.

24. Ishikawa, T., Aoyagi, H., Asaka, T., Asano, Y., Azumi, N., Bizen, T., Ego, H., Fukami, K., Fukui, T., Furukawa, Y., Goto, S., Hanaki, H., Hara, T., Hasegawa, T., Hatsui, T., Higashiya, A., Hirono, T., Hosoda, N., Ishii, M., Inagaki, T., Inubushi, Y., Itoga, T., Joti, Y., Kago, M., Kameshima, T., Kimura, H., Kirihara, Y., Kiyomichi, A., Kobayashi, T., Kondo, C., Kudo, T.,

Maesaka, H., Maréchal, X.M., Masuda, T., Matsubara, S., Matsumoto, T., Matsushita, T., Matsui, S., Nagasono, M., Nariyama, N., Ohashi, H., Ohata, T., Ohshima, T., Ono, S., Otake, Y., Saji, C., Sakurai, T., Sato, T., Sawada, K., Seike, T., Shirasawa, K., Sugimoto, T., Suzuki, S., Takahashi, S., Takebe, H., Takeshita, K., Tamasaku, K., Tanaka, H., Tanaka, R., Tanaka, T., Togashi, T., Togawa, K., Tokuhisa, A., Tomizawa, H., Tono, K., Wu, S., Yabashi, M., Yamaga, M., Yamashita, A., Yanagida, K., Zhang, C., Shintake, T., Kitamura, H., and Kumagai, N. (2012) A compact X-ray free-electron laser emitting in the sub-ångström region. *Nat. Photonics*, **6** (8), 540–544.

25. Nam, I., Min, C.-K., Oh, B., Kim, G., Na, D., Suh, Y.J., Yang, H., Cho, M.H., Kim, C., Kim, M.-J., Shim, C.H., Ko, J.H., Heo, H., Park, J., Kim, J., Park, S., Park, G., Kim, S., Chun, S.H., Hyun, H., Lee, J.H., Kim, K.S., Eom, I., Rah, S., Shu, D., Kim, K.-J., Terentyev, S., Blank, V., Shvyd'ko, Y., Lee, S.J., and Kang, H.-S. (2021) High-brightness self-seeded X-ray free-electron laser covering the 3.5 keV to 14.6 keV range. *Nat. Photonics*, **15** (6), 435–441.

26. Decking, W., Abeghyan, S., Abramian, P., Abramsky, A., Aguirre, A., Albrecht, C., Alou, P., Altarelli, M., Altmann, P., Amyan, K., Anashin, V., Apostolov, E., Appel, K., Auguste, D., Ayvazyan, V., Baark, S., Babies, F., Baboi, N., Bak, P., Balandin, V., Baldinger, R., Baranasic, B., Barbanotti, S., Belikov, O., Belokurov, V., Belova, L., Belyakov, V., Berry, S., Bertucci, M., Beutner, B., Block, A., Blöcher, M., Böckmann, T., Bohm, C., Böhnert, M., Bondar, V., Bondarchuk, E., Bonezzi, M., Borowiec, P., Bösch, C., Bösenberg, U., Bosotti, A., Böspflug, R., Bousonville, M., Boyd, E., Bozhko, Y., Brand, A., Branlard, J., Briechle, S., Brinker, F., Brinker, S., Brinkmann, R., Brockhauser, S., Brovko, O., Brück, H., Brüdgam, A., Butkowski, L., Büttner, T., Calero, J., Castro-Carballo, E., Cattalanotto, G., Charrier, J., Chen, J., Cherepenko, A., Cheskidov, V., Chiodini, M., Chong, A., Choroba, S., Chorowski, M., Churanov, D., Cichalewski, W., Clausen, M., Clement, W., Cloué, C., Cobos, J.A., Coppola, N., Cunis, S., Czuba, K., Czwalinna, M., D'Almagne, B., Dammann, J., Danared, H., de Zubiaurre Wagner, A., Delfs, A., Delfs, T., Dietrich, F., Dietrich, T., Dohlus, M., Dommach, M., Donat, A., Dong, X., Doynikov, N., Dressel, M., Duda, M., Duda, P., Eckoldt, H., Ehsan, W., Eidam, J., Eints, F., Engling, C., Englisch, U., Ermakov, A., Escherich, K., Eschke, J., Saldin, E., Faesing, M., Fallou, A., Felber, M., Fenner, M., Fernandes, B., Fernández, J.M., Feuker, S., Filippakopoulos, K., Floettmann, K., Fogel, V., Fontaine, M., Francés, A., Martin, I.F., Freund, W., Freyermuth, T., Friedland, M., Fröhlich, L., Fusetti, M., Fydrych, J., Gallas, A., García, O., Garcia-Tabares, L., Geloni, G., Gerasimova, N., Gerth, C., Geßler, P., Gharibyan, V., Gloor, M., Głowinkowski, J., Goessel, A., Gołębiewski, Z., Golubeva, N., Grabowski, W., Graeff, W., Grebentsov, A., Grecki, M., Grevsmuehl, T., Gross, M., Grosse-Wortmann, U., Grünert, J., Grunewald, S., Grzegory, P., Feng, G., Guler, H., Gusev, G., Gutierrez, J.L., Hagge, L., Hamberg, M., Hanneken, R., Harms, E., Hartl, I., Hauberg, A., Hauf, S., Hauschildt, J., Hauser, J., Havlicek, J., Hedqvist, A., Heidbrook, N., Hellberg, F., Henning, D., Hensler, O., Hermann, T., Hidvégi, A., Hierholzer, M., Hintz, H., Hoffmann, F., Hoffmann, M., Hoffmann, M., Holler, Y., Hüning, M., Ignatenko, A., Ilchen, M., Iluk, A., Iversen, J., Iversen, J., Izquierdo, M., Jachmann, L., Jardon, N., Jastrow, U., Jensch, K., Jensen, J., Jeżabek, M., Jidda, M., Jin, H., Johansson, N., Jonas, R., Kaabi, W.,

Kaefer, D., Kammering, R., Kapitza, H., Karabekyan, S., Karstensen, S., Kasprzak, K., Katalev, V., Keese, D., Keil, B., Kholopov, M., Killenberger, M., Kitaev, B., Klimchenko, Y., Klos, R., Knebel, L., Koch, A., Koepke, M., Köhler, S., Köhler, W., Kohlstrunk, N., Konopkova, Z., Konstantinov, A., Kook, W., Koprek, W., Körfer, M., Korth, O., Kosarev, A., Kosiński, K., Kostin, D., Kot, Y., Kotarba, A., Kozak, T., Kozak, V., Kramert, R., Krasilnikov, M., Krasnov, A., Krause, B., Kravchuk, L., Krebs, O., Kretschmer, R., Kreutzkamp, J., Kröplin, O., Krzysik, K., Kube, G., Kuehn, H., Kujala, N., Kulikov, V., Kuzminych, V., La Civita, D., Lacroix, M., Lamb, T., Lancetov, A., Larsson, M., Le Pinvidic, D., Lederer, S., Lensch, T., Lenz, D., Leuschner, A., Levenhagen, F., Li, Y., Liebing, J., Lilje, L., Limberg, T., Lipka, D., List, B., Liu, J., Liu, S., Lorbeer, B., Lorkiewicz, J., Lu, H.H., Ludwig, F., Machau, K., Maciocha, W., Madec, C., Magueur, C., Maiano, C., Maksimova, I., Malcher, K., Maltezopoulos, T., Mamoshkina, E., Manschwetus, B., Marcellini, F., Marinkovic, G., Martinez, T., Martirosyan, H., Maschmann, W., Maslov, M., Matheisen, A., Mavric, U., Meißner, J., Meissner, K., Messerschmidt, M., Meyners, N., Michalski, G., Michelato, P., Mildner, N., Moe, M., Moglia, F., Mohr, C., Mohr, S., Möller, W., Mommerz, M., Monaco, L., Montiel, C., Moretti, M., Morozov, I., Morozov, P., Mross, D., Mueller, J., Müller, C., Müller, J., Müller, K., Munilla, J., Münnich, A., Muratov, V., Napoly, O., Näser, B., Nefedov, N., Neumann, R., Neumann, R., Ngada, N., Noelle, D., Obier, F., Okunev, I., Oliver, J.A., Omet, M., Oppelt, A., Ottmar, A., Oublaid, M., Pagani, C., Paparella, R., Paramonov, V., Peitzmann, C., Penning, J., Perus, A., Peters, F., Petersen, B., Petrov, A., Petrov, I., Pfeiffer, S., Pflüger, J., Philipp, S., Pienaud, Y., Pierini, P., Pivovarov, S., Planas, M., Pławski, E., Pohl, M., Polinski, J., Popov, V., Prat, S., Prenting, J., Priebe, G., Pryschelski, H., Przygoda, K., Pyata, E., Racky, B., Rathjen, A., Ratuschni, W., Regnaud-Campderros, S., Rehlich, K., Reschke, D., Robson, C., Roever, J., Roggli, M., Rothenburg, J., Rusiński, E., Rybaniec, R., Sahling, H., Salmani, M., Samoylova, L., Sanzone, D., Saretzki, F., Sawlanski, O., Schaffran, J., Schlarb, H., Schlösser, M., Schlott, V., Schmidt, C., Schmidt-Foehre, F., Schmitz, M., Schmökel, M., Schnautz, T., Schneidmiller, E., Scholz, M., Schöneburg, B., Schultze, J., Schulz, C., Schwarz, A., Sekutowicz, J., Sellmann, D., Semenov, E., Serkez, S., Sertore, D., Shehzad, N., Shemarykin, P., Shi, L., Sienkiewicz, M., Sikora, D., Sikorski, M., Silenzi, A., Simon, C., Singer, W., Singer, X., Sinn, H., Sinram, K., Skvorodnev, N., Smirnow, P., Sommer, T., Sorokin, A., Stadler, M., Steckel, M., Steffen, B., Steinhau-Kühl, N., Stephan, F., Stodulski, M., Stolper, M., Sulimov, A., Susen, R., Świerblewski, J., Sydlo, C., Syresin, E., Sytchev, V., Szuba, J., Tesch, N., Thie, J., Thiebault, A., Tiedtke, K., Tischhauser, D., Tolkiehn, J., Tomin, S., Tonisch, F., Toral, F., Torbin, I., Trapp, A., Treyer, D., Trowitzsch, G., Trublet, T., Tschentscher, T., Ullrich, F., Vannoni, M., Varela, P., Varghese, G., Vashchenko, G., Vasic, M., Vazquez-Velez, C., Verguet, A., Vilcins-Czvitkovits, S., Villanueva, R., Visentin, B., Viti, M., Vogel, E., Volobuev, E., Wagner, R., Walker, N., Wamsat, T., Weddig, H., Weichert, G., Weise, H., Wenndorf, R., Werner, M., Wichmann, R., Wiebers, C., Wiencek, M., Wilksen, T., Will, I., Winkelmann, L., Winkowski, M., Wittenburg, K., Witzig, A., Wlk, P., Wohlenberg, T., Wojciechowski, M., Wolff-Fabris, F., Wrochna, G., Wrona, K., Yakopov, M., Yang, B., Yang, F., Yurkov, M., Zagorodnov, I.,

Zalden, P., Zavadtsev, A., Zavadtsev, D., Zhirnov, A., Zhukov, A., Ziemann, V., Zolotov, A., Zolotukhina, N., Zummack, F., and Zybin, D. (2020) A MHz-repetition-rate hard X-ray free-electron laser driven by a superconducting linear accelerator. *Nat. Photonics*, **14** (6), 391–397.

27. Liu, B., Feng, C., Gu, D., Gao, F., Deng, H., Zhang, M., Sun, S., Chen, S., Zhang, W., Fang, W., Wang, Z., Zhou, Q., Leng, Y., Gu, M., Yin, L., Gu, Q., Fang, G., Wang, D., and Zhao, Z. (2021) The SXFEL Upgrade: From Test Facility to User Facility. *Appl. Sci.*, **12** (1), 176.
28. Zhu, Z.U., Zhao, Z.T., Wang, D., Liu, Z., Li, R.X., Yin, L.X., and Yang, Z.H. (2017) SCLF: An 8-GeV CW SCRF LINAC-Based X-Ray FEL Facility in Shanghai. *Proc FEL2017*.
29. Stolow, A., Bragg, A.E., and Neumark, D.M. (2004) Femtosecond Time-Resolved Photoelectron Spectroscopy. *Chem. Rev.*, **104** (4), 1719–1758.
30. Boll, R., Schäfer, J.M., Richard, B., Fehre, K., Kastirke, G., Jurek, Z., Schöffler, M.S., Abdullah, M.M., Anders, N., Baumann, T.M., Eckart, S., Erk, B., De Fanis, A., Dörner, R., Grundmann, S., Grychtol, P., Hartung, A., Hofmann, M., Ilchen, M., Inhester, L., Janke, C., Jin, R., Kircher, M., Kubicek, K., Kunitski, M., Li, X., Mazza, T., Meister, S., Melzer, N., Montano, J., Music, V., Nalin, G., Ovcharenko, Y., Passow, C., Pier, A., Rennhack, N., Rist, J., Rivas, D.E., Rolles, D., Schlichting, I., Schmidt, L.Ph.H., Schmidt, P., Siebert, J., Strenger, N., Trabert, D., Trinter, F., Vela-Perez, I., Wagner, R., Walter, P., Weller, M., Ziolkowski, P., Son, S.-K., Rudenko, A., Meyer, M., Santra, R., and Jahnke, T. (2022) X-ray multiphoton-induced Coulomb explosion images complex single molecules. *Nat. Phys.*, **18** (4), 423–428.
31. Pitzer, M., Kunitski, M., Johnson, A.S., Jahnke, T., Sann, H., Sturm, F., Schmidt, L.Ph.H., Schmidt-Böcking, H., Dörner, R., Stohner, J., Kiedrowski, J., Reggelin, M., Marquardt, S., Schießer, A., Berger, R., and Schöffler, M.S. (2013) Direct Determination of Absolute Molecular Stereochemistry in Gas Phase by Coulomb Explosion Imaging. *Science*, **341** (6150), 1096–1100.
32. Vager, Z., Naaman, R., and Kanter, E.P. (1989) Coulomb Explosion Imaging of Small Molecules. *Science*, **244** (4903), 426–431.
33. Giussani, A., Segarra-Martí, J., Roca-Sanjuán, D., and Merchán, M. (2013) Excitation of Nucleobases from a Computational Perspective I: Reaction Paths, in *Photoinduced Phenomena in Nucleic Acids I*, vol. 355, Springer International Publishing, Cham, pp. 57–97.
34. Mai, S., Richter, M., Marquetand, P., and González, L. (2014) Excitation of Nucleobases from a Computational Perspective II: Dynamics, in *Photoinduced Phenomena in Nucleic Acids I*, vol. 355, Springer International Publishing, Cham, pp. 99–153.
35. Curchod, B.F.E., and Martínez, T.J. (2018) Ab Initio Nonadiabatic Quantum Molecular Dynamics. *Chem. Rev.*, **118** (7), 3305–3336.
36. Daniels, M., and Hauswirth, W. (1971) Fluorescence of the Purine and Pyrimidine Bases of the Nucleic Acids in Neutral Aqueous Solution at 300 K. *Science*, **171** (3972), 675–677.

37. González-Vázquez, J., González, L., Samoylova, E., and Schultz, T. (2009) Thymine relaxation after UV irradiation: the role of tautomerization and πσ* states. *Phys. Chem. Chem. Phys.*, **11** (20), 3927.
38. Feyer, V., Plekan, O., Richter, R., Coreno, M., Vall-llosera, G., Prince, K.C., Trofimov, A.B., Zaytseva, I.L., Moskovskaya, T.E., Gromov, E.V., and Schirmer, J. (2009) Tautomerism in Cytosine and Uracil: An Experimental and Theoretical Core Level Spectroscopic Study. *J. Phys. Chem. A*, **113** (19), 5736–5742.
39. McFarland, B.K., Farrell, J.P., Miyabe, S., Tarantelli, F., Aguilar, A., Berrah, N., Bostedt, C., Bozek, J.D., Bucksbaum, P.H., Castagna, J.C., Coffee, R.N., Cryan, J.P., Fang, L., Feifel, R., Gaffney, K.J., Glownia, J.M., Martinez, T.J., Mucke, M., Murphy, B., Natan, A., Osipov, T., Petrović, V.S., Schorb, S., Schultz, Th., Spector, L.S., Swiggers, M., Tenney, I., Wang, S., White, J.L., White, W., and Gühr, M. (2014) Ultrafast X-ray Auger probing of photoexcited molecular dynamics. *Nat. Commun.*, **5** (May), 4235.
40. Hare, P.M., Crespo-Hernández, C.E., and Kohler, B. (2007) Internal conversion to the electronic ground state occurs via two distinct pathways for pyrimidine bases in aqueous solution. *Proc. Natl. Acad. Sci.*, **104** (2), 435–440.
41. Asturiol, D., Lasorne, B., Robb, M.A., and Blancafort, L. (2009) Photophysics of the π,π* and n,π* States of Thymine: MS-CASPT2 Minimum-Energy Paths and CASSCF on-the-Fly Dynamics. *J. Phys. Chem. A*, **113** (38), 10211–10218.
42. Nakayama, A., Arai, G., Yamazaki, S., and Taketsugu, T. (2013) Solvent effects on the ultrafast nonradiative deactivation mechanisms of thymine in aqueous solution: Excited-state QM/MM molecular dynamics simulations. *J. Chem. Phys.*, **139** (21), 214304.
43. Barbatti, M., Aquino, A.J.A., and Lischka, H. (2010) The UV absorption of nucleobases: Semi-classical ab initio spectra simulations. *Phys. Chem. Chem. Phys.*, **12** (19), 4959–4967.
44. Picconi, D., Barone, V., Lami, A., Santoro, F., and Improta, R. (2011) The Interplay between ππ*/nπ* Excited States in Gas-Phase Thymine: A Quantum Dynamical Study. *ChemPhysChem*, **12** (10), 1957–1968.
45. Reuther, A., Iglev, H., Laenen, R., and Laubereau, A. (2000) Femtosecond photo-ionization of nucleic acid bases: electronic lifetimes and electron yields. *Chem. Phys. Lett.*, **325** (4), 360–368.
46. Gustavsson, T., Sharonov, A., and Markovitsi, D. (2002) Thymine, thymidine and thymidine 5'-monophosphate studied by femtosecond fluorescence upconversion spectroscopy. *Chem. Phys. Lett.*, **351** (3–4), 195–200.
47. Gustavsson, T., Bányász, Á., Lazzarotto, E., Markovitsi, D., Scalmani, G., Frisch, M.J., Barone, V., and Improta, R. (2006) Singlet Excited-State Behavior of Uracil and Thymine in Aqueous Solution: A Combined Experimental and Computational Study of 11 Uracil Derivatives. *J. Am. Chem. Soc.*, **128** (2), 607–619.
48. Hare, P.M., Middleton, C.T., Mertel, K.I., Herbert, J.M., and Kohler, B. (2008) Time-resolved infrared spectroscopy of the lowest triplet state of thymine and thymidine. *Chem. Phys.*, **347** (1–3), 383–392.

49. Buchner, F., Nakayama, A., Yamazaki, S., Ritze, H.-H., and Lübcke, A. (2015) Excited-State Relaxation of Hydrated Thymine and Thymidine Measured by Liquid-Jet Photoelectron Spectroscopy: Experiment and Simulation. *J. Am. Chem. Soc.*, **137** (8), 2931–2938.
50. Manna, A., Park, S., Lee, T., and Lim, M. (2016) Photoexcitation Dynamics of Thymine in Acetonitrile and an Ionic Liquid Probed by Time-resolved Infrared Spectroscopy: Photoexcitation Dynamics of Thymine. *Bull. Korean Chem. Soc.*, **37** (7), 1064–1070.
51. Miura, Y., Yamamoto, Y., Karashima, S., Orimo, N., Hara, A., Fukuoka, K., Ishiyama, T., and Suzuki, T. (2023) Formation of Long-Lived Dark States during Electronic Relaxation of Pyrimidine Nucleobases Studied Using Extreme Ultraviolet Time-Resolved Photoelectron Spectroscopy. *J. Am. Chem. Soc.*, **145** (6), 3369–3381.
52. Kang, H., Lee, K.T., Jung, B., Ko, Y.J., and Kim, S.K. (2002) Intrinsic Lifetimes of the Excited State of DNA and RNA Bases. *J. Am. Chem. Soc.*, **124** (44), 12958–12959.
53. He, Y., Wu, C., and Kong, W. (2003) Decay Pathways of Thymine and Methyl-Substituted Uracil and Thymine in the Gas Phase. *J. Phys. Chem. A*, **107** (26), 5145–5148.
54. Ligare, M., Siouri, F., Bludsky, O., Nachtigallová, D., and De Vries, M.S. (2015) Characterizing the dark state in thymine and uracil by double resonant spectroscopy and quantum computation. *Phys. Chem. Chem. Phys.*, **17** (37), 24336–24341.
55. Yu, H., Sanchez-Rodriguez, J.A., Pollum, M., Crespo-Hernández, C.E., Mai, S., Marquetand, P., González, L., and Ullrich, S. (2016) Internal conversion and intersystem crossing pathways in UV excited, isolated uracils and their implications in prebiotic chemistry. *Phys. Chem. Chem. Phys.*, **18** (30), 20168–20176.
56. Canuel, C., Mons, M., Piuzzi, F., Tardivel, B., Dimicoli, I., and Elhanine, M. (2005) Excited states dynamics of DNA and RNA bases: Characterization of a stepwise deactivation pathway in the gas phase. *J. Chem. Phys.*, **122** (7), 074316.
57. Wolf, T.J.A., Parrish, R.M., Myhre, R.H., Martínez, T.J., Koch, H., and Gühr, M. (2019) Observation of Ultrafast Intersystem Crossing in Thymine by Extreme Ultraviolet Time-Resolved Photoelectron Spectroscopy. *J. Phys. Chem. A*, **123** (32), 6897–6903.
58. Ullrich, S., Schultz, T., Zgierski, M.Z., and Stolow, A. (2004) Direct Observation of Electronic Relaxation Dynamics in Adenine via Time-Resolved Photoelectron Spectroscopy. *J. Am. Chem. Soc.*, **126** (8), 2262–2263.
59. Ghafur, O., Crane, S.W., Ryszka, M., Bockova, J., Rebelo, A., Saalbach, L., De Camillis, S., Greenwood, J.B., Eden, S., and Townsend, D. (2018) Ultraviolet relaxation dynamics in uracil: Time-resolved photoion yield studies using a laser-based thermal desorption source. *J. Chem. Phys.*, **149** (3), 034301.
60. Koyama, D., Milner, M.J., and Orr-Ewing, A.J. (2017) Evidence for a Double Well in the First Triplet Excited State of 2-Thiouracil. *J. Phys. Chem. B*, **121** (39), 9274–9280.
61. Mai, S., Mohamadzade, A., Marquetand, P., González, L., and Ullrich, S. (2018) Simulated and Experimental Time-Resolved Photoelectron Spectra of the Intersystem Crossing Dynamics in 2-Thiouracil. *Molecules*, **23** (11), 2836.
62. Pollum, M., Martínez-Fernández, L., and Crespo-Hernández, C.E. (2014)

Photochemistry of Nucleic Acid Bases and Their Thio- and Aza-Analogues in Solution, in *Photoinduced Phenomena in Nucleic Acids I*, vol. 355, Springer International Publishing, Cham, pp. 245–327.
63. Teles-Ferreira, D.C., Conti, I., Borrego-Varillas, R., Nenov, A., Van Stokkum, I.H.M., Ganzer, L., Manzoni, C., Paula, A.M., Cerullo, G., and Garavelli, M. (2020) A Unified Experimental/Theoretical Description of the Ultrafast Photophysics of Single and Double Thionated Uracils. *Chem. – Eur. J.*, **26** (1), 336–343.
64. Robinson, M.S., Niebuhr, M., and Gühr, M. (2023) Ultrafast Photo-Ion Probing of the Relaxation Dynamics in 2-Thiouracil. *Molecules*, **28** (5), 2354.
65. Sánchez-Rodríguez, J.A., Mohamadzade, A., Mai, S., Ashwood, B., Pollum, M., Marquetand, P., González, L., Crespo-Hernández, C.E., and Ullrich, S. (2017) 2-Thiouracil intersystem crossing photodynamics studied by wavelength-dependent photoelectron and transient absorption spectroscopies. *Phys. Chem. Chem. Phys.*, **19** (30), 19756–19766.
66. Mai, S., Marquetand, P., and González, L. (2015) A Static Picture of the Relaxation and Intersystem Crossing Mechanisms of Photoexcited 2-Thiouracil. *J. Phys. Chem. A*, **119** (36), 9524–9533.
67. Mayer, D., Picconi, D., Robinson, M.S., and Gühr, M. (2022) Experimental and theoretical gas-phase absorption spectra of thionated uracils. *Chem. Phys.*, **558** (March), 111500.
68. Mai, S., Marquetand, P., and González, L. (2016) Intersystem Crossing Pathways in the Noncanonical Nucleobase 2-Thiouracil: A Time-Dependent Picture. *J. Phys. Chem. Lett.*, **7** (11), 1978–1983.
69. Mai, S., Plasser, F., Pabst, M., Neese, F., Köhn, A., and González, L. (2017) Surface hopping dynamics including intersystem crossing using the algebraic diagrammatic construction method. *J. Chem. Phys.*, **147** (18), 184109.
70. Cui, G., and Fang, W. (2013) State-specific heavy-atom effect on intersystem crossing processes in 2-thiothymine: A potential photodynamic therapy photosensitizer. *J. Chem. Phys.*, **138** (4), 044315.
71. Siegbahn, K. (1969) *ESCA applied to free molecules*, North-Holland Pub. Co, Amsterdam.
72. Gelius, U. (1974) Binding Energies and Chemical Shifts in ESCA. *Phys. Scr.*, **9** (3), 133–147.
73. Travnikova, O., Borve, K.J., Patanen, M., Söderström, J., Miron, C., Saethre, L.J., Martensson, N., and Svensson, S. (2012) The ESCA molecule—Historical remarks and new results. *J. Electron Spectrosc. Relat. Phenom.*, **185** (8–9), 191–197.
74. Plekan, O., Feyer, V., Richter, R., Coreno, M., de Simone, M., Prince, K.C., Trofimov, A.B., Gromov, E.V., Zaytseva, I.L., and Schirmer, J. (2008) A theoretical and experimental study of the near edge X-ray absorption fine structure (NEXAFS) and X-ray photoelectron spectra (XPS) of nucleobases: Thymine and adenine. *Chem. Phys.*, **347** (1–3), 360–375.
75. Giuliano, B.M., Feyer, V., Prince, K.C., Coreno, M., Evangelisti, L., Melandri, S., and Caminati, W. (2010) Tautomerism in 4-Hydroxypyrimidine, *S* -Methyl-2-thiouracil, and 2-

912 Thiouracil. *J. Phys. Chem. A*, **114** (48), 12725–12730.
913 76. Stöhr, J. (1996) *NEXAFS spectroscopy*, Springer, Berlin ; New York.
914 77. Meitner, L. (1922) Uber die Entstehung der Beta-Strahl-Spektren radioaktiver
915 Substanzen. *Z. Fuer Phys.*, **9** (1), 131–144.
916 78. PierreAuger (1923) Sur les rayons beta; secondaires produits dans un gaz par des
917 rayons X. *C.R.A.S.*, **177**, 169–171.
918 79. Yong, H., Moreno Carrascosa, A., Ma, L., Stankus, B., Minitti, M.P., Kirrander, A., and
919 Weber, P.M. (2021) Determination of excited state molecular structures from time-
920 resolved gas-phase X-ray scattering. *Faraday Discuss.*, **228**, 104–122.
921 80. Yong, H., Xu, X., Ruddock, J.M., Stankus, B., Carrascosa, A.M., Zotev, N., Bellshaw, D.,
922 Du, W., Goff, N., Chang, Y., Boutet, S., Carbajo, S., Koglin, J.E., Liang, M., Robinson, J.S.,
923 Kirrander, A., Minitti, M.P., and Weber, P.M. (2021) Ultrafast X-ray scattering offers a
924 structural view of excited-state charge transfer. *Proc. Natl. Acad. Sci.*, **118** (19),
925 e2021714118.
926 81. Minitti, M.P., Budarz, J.M., Kirrander, A., Robinson, J., Lane, T.J., Ratner, D., Saita, K.,
927 Northey, T., Stankus, B., Cofer-Shabica, V., Hastings, J., and Weber, P.M. (2014) Toward
928 structural femtosecond chemical dynamics: imaging chemistry in space and time. *Faraday*
929 *Discuss*, **171**, 81–91.
930 82. Stankus, B., Yong, H., Zotev, N., Ruddock, J.M., Bellshaw, D., Lane, T.J., Liang, M.,
931 Boutet, S., Carbajo, S., Robinson, J.S., Du, W., Goff, N., Chang, Y., Koglin, J.E., Minitti, M.P.,
932 Kirrander, A., and Weber, P.M. (2019) Ultrafast X-ray scattering reveals vibrational
933 coherence following Rydberg excitation. *Nat. Chem.*, **11** (8), 716–721.
934 83. Küpper, J., Stern, S., Holmegaard, L., Filsinger, F., Rouzée, A., Rudenko, A., Johnsson,
935 P., Martin, A.V., Adolph, M., Aquila, A., Bajt, S., Barty, A., Bostedt, C., Bozek, J., Caleman,
936 C., Coffee, R., Coppola, N., Delmas, T., Epp, S., Erk, B., Foucar, L., Gorkhover, T.,
937 Gumprecht, L., Hartmann, A., Hartmann, R., Hauser, G., Holl, P., Hömke, A., Kimmel, N.,
938 Krasniqi, F., Kühnel, K.-U., Maurer, J., Messerschmidt, M., Moshammer, R., Reich, C.,
939 Rudek, B., Santra, R., Schlichting, I., Schmidt, C., Schorb, S., Schulz, J., Soltau, H., Spence,
940 J.C.H., Starodub, D., Strüder, L., Thøgersen, J., Vrakking, M.J.J., Weidenspointner, G.,
941 White, T.A., Wunderer, C., Meijer, G., Ullrich, J., Stapelfeldt, H., Rolles, D., and Chapman,
942 H.N. (2014) X-Ray Diffraction from Isolated and Strongly Aligned Gas-Phase Molecules
943 with a Free-Electron Laser. *Phys. Rev. Lett.*, **112** (8), 083002.
944 84. Yang, J., Zhu, X., Wolf, T.J.A., Li, Z., Nunes, J.P.F., Coffee, R., Cryan, J.P., Gühr, M.,
945 Hegazy, K., Heinz, T.F., Jobe, K., Li, R., Shen, X., Veccione, T., Weathersby, S., Wilkin, K.J.,
946 Yoneda, C., Zheng, Q., Martinez, T.J., Centurion, M., and Wang, X. (2018) Imaging CF_3I
947 conical intersection and photodissociation dynamics with ultrafast electron diffraction.
948 *Science*, **361** (6397), 64–67.
949 85. Wolf, T.J.A., Sanchez, D.M., Yang, J., Parrish, R.M., Nunes, J.P.F., Centurion, M.,
950 Coffee, R., Cryan, J.P., Gühr, M., Hegazy, K., Kirrander, A., Li, R.K., Ruddock, J., Shen, X.,
951 Vecchione, T., Weathersby, S.P., Weber, P.M., Wilkin, K., Yong, H., Zheng, Q., Wang, X.J.,
952 Minitti, M.P., and Martínez, T.J. (2018) Imaging the Photochemical Ring-Opening of 1,3-

Cyclohexadiene by Ultrafast Electron Diffraction. *Nat. Chem.*, **11** (6), 504–509.
86. Yang, J., Guehr, M., Vecchione, T., Robinson, M.S., Li, R., Hartmann, N., Shen, X., Coffee, R., Corbett, J., Fry, A., Gaffney, K., Gorkhover, T., Hast, C., Jobe, K., Makasyuk, I., Reid, A., Robinson, J., Vetter, S., Wang, F., Weathersby, S., Yoneda, C., Centurion, M., and Wang, X. (2016) Diffractive imaging of a rotational wavepacket in nitrogen molecules with femtosecond megaelectronvolt electron pulses. *Nat. Comm*, **7**, 11232.
87. Yang, J., Guehr, M., Shen, X., Li, R., Vecchione, T., Coffee, R., Corbett, J., Fry, A., Hartmann, N., Hast, C., Hegazy, K., Jobe, K., Makasyuk, I., Robinson, J., Robinson, M.S., Vetter, S., Weathersby, S., Yoneda, C., Wang, X., and Centurion, M. (2016) Diffractive Imaging of Coherent Nuclear Motion in Isolated Molecules. *Phys. Rev. Lett.*, **117** (15), 173002.
88. Plönjes, E., Faatz, B., Kuhlmann, M., and Treusch, R. (2016) FLASH2: Operation, beamlines, and photon diagnostics. *AIP Conf. Proc.*, **1741**, 20008.
89. Faatz, B., Braune, M., Hensler, O., Honkavaara, K., Kammering, R., Kuhlmann, M., Ploenjes, E., Roensch-Schulenburg, J., Schneidmiller, E., Schreiber, S., Tiedtke, K., Tischer, M., Treusch, R., Vogt, M., Wurth, W., Yurkov, M., and Zemella, J. (2017) The FLASH Facility: Advanced Options for FLASH2 and Future Perspectives. *Appl. Sci.*, **7** (11), 1114.
90. McFarland, B.K., Berrah, N., Bostedt, C., Bozek, J., Bucksbaum, P.H., Castagna, J.C., Coffee, R.N., Cryan, J.P., Fang, L., Farrell, J.P., Feifel, R., Gaffney, K.J., Glownia, J.M., Martinez, T.J., Miyabe, S., Mucke, M., Murphy, B., Natan, A., Osipov, T., Petrovic, V.S., Schorb, S., Schultz, T., Spector, L.S., Swiggers, M., Tarantelli, F., Tenney, I., Wang, S., White, J.L., White, W., and Gühr, M. (2014) Experimental strategies for optical pump – soft x-ray probe experiments at the LCLS. *J. Phys. Conf. Ser.*, **488** (1), 012015.
91. Metje, J., Lever, F., Mayer, D., Squibb, R.J., Robinson, M.S., Niebuhr, M., Feifel, R., Düsterer, S., and Gühr, M. (2020) URSA-PQ: A Mobile and Flexible Pump-Probe Instrument for Gas Phase Samples at the FLASH Free Electron Laser. *Appl. Sci.*, **10** (21), 7882.
92. Kruit, P., and Read, F.H. (1983) Magnetic field paralleliser for 2π electron-spectrometer and electron-image magnifier. *J. Phys. [E]*, **16** (4), 313–324.
93. Wolf, T.J.A., Myhre, R.H., Cryan, J.P., Coriani, S., Squibb, R.J., Battistoni, A., Berrah, N., Bostedt, C., Bucksbaum, P., Coslovich, G., Feifel, R., Gaffney, K.J., Grilj, J., Martinez, T.J., Miyabe, S., Moeller, S.P., Mucke, M., Natan, A., Obaid, R., Osipov, T., Plekan, O., Wang, S., Koch, H., and Gühr, M. (2017) Probing ultrafast ππ*/nπ* internal conversion in organic chromophores via K-edge resonant absorption. *Nat. Commun.*, **1610.08498** (1), 1–6.
94. Loh, Z.-H., Doumy, G., Arnold, C., Kjellsson, L., Southworth, S.H., Al Haddad, A., Kumagai, Y., Tu, M.-F., Ho, P.J., March, A.M., Schaller, R.D., Bin Mohd Yusof, M.S., Debnath, T., Simon, M., Welsch, R., Inhester, L., Khalili, K., Nanda, K., Krylov, A.I., Moeller, S., Coslovich, G., Koralek, J., Minitti, M.P., Schlotter, W.F., Rubensson, J.-E., Santra, R., and Young, L. (2020) Observation of the fastest chemical processes in the radiolysis of water. *Science*, **367** (6474), 179–182.

95. Szymczak, J.J., Barbatti, M., Soo Hoo, J.T., Adkins, J.A., Windus, T.L., Nachtigallová, D., and Lischka, H. (2009) Photodynamics Simulations of Thymine: Relaxation into the First Excited Singlet State †. *J. Phys. Chem. A*, **113** (45), 12686–12693.
96. Bressler, C., and Chergui, M. (2004) Ultrafast X-ray Absorption Spectroscopy. *Chem. Rev.*, **104** (4), 1781–1812.
97. Zhang, W., Alonso-Mori, R., Bergmann, U., Bressler, C., Chollet, M., Galler, A., Gawelda, W., Hadt, R.G., Hartsock, R.W., Kroll, T., Kjær, K.S., Kubiček, K., Lemke, H.T., Liang, H.W., Meyer, D.A., Nielsen, M.M., Purser, C., Robinson, J.S., Solomon, E.I., Sun, Z., Sokaras, D., van Driel, T.B., Vankó, G., Weng, T.-C., Zhu, D., and Gaffney, K.J. (2014) Tracking excited-state charge and spin dynamics in iron coordination complexes. *Nature*, **509** (7500), 345–348.
98. Attar, A.R., Bhattacherjee, A., Pemmaraju, C.D., Schnorr, K., Closser, K.D., Prendergast, D., and Leone, S.R. (2017) Femtosecond x-ray spectroscopy of an electrocyclic ring-opening reaction. *Science*, **356** (6333), 54–59.
99. Bhattacherjee, A., Pemmaraju, C.D., Schnorr, K., Attar, A.R., and Leone, S.R. (2017) Ultrafast Intersystem Crossing in Acetylacetone via Femtosecond X-ray Transient Absorption at the Carbon K-Edge. *J. Am. Chem. Soc.*, **139** (46), 16576–16583.
100. Pertot, Y., Schmidt, C., Matthews, M., Chauvet, A., Huppert, M., Svoboda, V., von Conta, A., Tehlar, A., Baykusheva, D., Wolf, J.-P., and Wörner, H.J. (2017) Time-resolved x-ray absorption spectroscopy with a water window high-harmonic source. *Science*, **355** (6322), 264–267.
101. Zinchenko, K.S., Ardana-Lamas, F., Seidu, I., Neville, S.P., Van Der Veen, J., Lanfaloni, V.U., Schuurman, M.S., and Wörner, H.J. (2021) Sub-7-femtosecond conical-intersection dynamics probed at the carbon K-edge. *Science*, **371** (6528), 489–494.
102. Mayer, D., Lever, F., Picconi, D., Metje, J., Alisauskas, S., Calegari, F., Düsterer, S., Ehlert, C., Feifel, R., Niebuhr, M., Manschwetus, B., Kuhlmann, M., Mazza, T., Robinson, M.S., Squibb, R.J., Trabattoni, A., Wallner, M., Saalfrank, P., Wolf, T.J.A., and Gühr, M. (2022) Following excited-state chemical shifts in molecular ultrafast x-ray photoelectron spectroscopy. *Nat. Commun.*, **13** (1), 198.
103. Leitner, T., Josefsson, I., Mazza, T., Miedema, P.S., Schröder, H., Beye, M., Kunnus, K., Schreck, S., Düsterer, S., Föhlisch, A., Meyer, M., Odelius, M., and Wernet, Ph. (2018) Time-resolved electron spectroscopy for chemical analysis of photodissociation: Photoelectron spectra of $Fe(CO)_5$, $Fe(CO)_4$, and $Fe(CO)_3$. *J. Chem. Phys.*, **149** (4), 044307.
104. Braußе, F., Goldsztejn, G., Amini, K., Boll, R., Bari, S., Bomme, C., Brouard, M., Burt, M., de Miranda, B.C., Düsterer, S., Erk, B., Géléoc, M., Geneaux, R., Gentleman, A.S., Guillemin, R., Ismail, I., Johnsson, P., Journel, L., Kierspel, T., Köckert, H., Küpper, J., Lablanquie, P., Lahl, J., Lee, J.W.L., Mackenzie, S.R., Maclot, S., Manschwetus, B., Mereshchenko, A.S., Mullins, T., Olshin, P.K., Palaudoux, J., Patchkovskii, S., Penent, F., Piancastelli, M.N., Rompotis, D., Ruchon, T., Rudenko, A., Savelyev, E., Schirmel, N., Techert, S., Travnikova, O., Trippel, S., Underwood, J.G., Vallance, C., Wiese, J., Simon, M.,

Holland, D.M.P., Marchenko, T., Rouzée, A., and Rolles, D. (2018) Time-resolved inner-shell photoelectron spectroscopy: From a bound molecule to an isolated atom. *Phys. Rev. A*, **97** (4), 043429.

105. Allum, F., Music, V., Inhester, L., Boll, R., Erk, B., Schmidt, P., Baumann, T.M., Brenner, G., Burt, M., Demekhin, P.V., Dörner, S., Ehresmann, A., Galler, A., Grychtol, P., Heathcote, D., Kargin, D., Larsson, M., Lee, J.W.L., Li, Z., Manschwetus, B., Marder, L., Mason, R., Meyer, M., Otto, H., Passow, C., Pietschnig, R., Ramm, D., Schubert, K., Schwob, L., Thomas, R.D., Vallance, C., Vidanović, I., von Korff Schmising, C., Wagner, R., Walter, P., Zhaunerchyk, V., Rolles, D., Bari, S., Brouard, M., and Ilchen, M. (2022) A localized view on molecular dissociation via electron-ion partial covariance. *Commun. Chem.*, **5** (1).

106. Faccialà, D., Devetta, M., Beauvarlet, S., Besley, N., Calegari, F., Callegari, C., Catone, D., Cinquanta, E., Ciriolo, A.G., Colaizzi, L., Coreno, M., Crippa, G., De Ninno, G., Di Fraia, M., Galli, M., Garcia, G.A., Mairesse, Y., Negro, M., Plekan, O., Prasannan Geetha, P., Prince, K.C., Pusala, A., Stagira, S., Turchini, S., Ueda, K., You, D., Zema, N., Blanchet, V., Nahon, L., Powis, I., and Vozzi, C. (2023) Time-Resolved Chiral X-Ray Photoelectron Spectroscopy with Transiently Enhanced Atomic Site Selectivity: A Free-Electron Laser Investigation of Electronically Excited Fenchone Enantiomers. *Phys. Rev. X*, **13** (1), 011044.

107. Gabalski, I., Allum, F., Seidu, I., Britton, M., Brenner, G., Bromberger, H., Brouard, M., Bucksbaum, P.H., Burt, M., Cryan, J.P., Driver, T., Ekanayake, N., Erk, B., Garg, D., Gougoula, E., Heathcote, D., Hockett, P., Holland, D.M.P., Howard, A.J., Kumar, S., Lee, J.W.L., Li, S., McManus, J., Mikosch, J., Milesevic, D., Minns, R.S., Neville, S., Atia-Tul-Noor, Papadopoulou, C.C., Passow, C., Razmus, W.O., Röder, A., Rouzée, A., Simao, A., Unwin, J., Vallance, C., Walmsley, T., Wang, J., Rolles, D., Stolow, A., Schuurman, M.S., and Forbes, R. (2023) Time-Resolved X-ray Photoelectron Spectroscopy: Ultrafast Dynamics in CS_2 Probed at the S 2p Edge. *J. Phys. Chem. Lett.*, **14** (31), 7126–7133.

108. Lever, F., Mayer, D., Picconi, D., Metje, J., Alisauskas, S., Calegari, F., Düsterer, S., Ehlert, C., Feifel, R., Niebuhr, M., Manschwetus, B., Kuhlmann, M., Mazza, T., Robinson, M.S., Squibb, R.J., Trabattoni, A., Wallner, M., Saalfrank, P., Wolf, T.J.A., and Gühr, M. (2020) Ultrafast dynamics of 2-thiouracil investigated by time-resolved Auger spectroscopy. *J. Phys. B At. Mol. Opt. Phys.*, **54** (1), 014002.

109. Wolf, T.J.A., Paul, A.C., Folkestad, S.D., Myhre, R.H., Cryan, J.P., Berrah, N., Bucksbaum, P.H., Coriani, S., Coslovich, G., Feifel, R., Martinez, T.J., Moeller, S.P., Mucke, M., Obaid, R., Plekan, O., Squibb, R.J., Koch, H., and Gühr, M. (2021) Transient resonant Auger–Meitner spectra of photoexcited thymine. *Faraday Discuss.*, **228**, 10.1039.D0FD00112K.

110. Dörner, R., Mergel, V., Jagutzki, O., Spielberger, L., Ullrich, J., Moshammer, R., and Schmidt-Böcking, H. (2000) Cold Target Recoil Ion Momentum Spectroscopy: a "momentum microscope" to view atomic collision dynamics. *Phys. Rep.*, **330** (2–3), 95–192.

111. Ullrich, J., Moshammer, R., Dörner, R., Jagutzki, O., Mergel, V., Schmidt-Böcking, H., and Spielberger, L. (1997) Recoil-ion momentum spectroscopy. *J. Phys. B*, **30** (13), 2917–2974.
112. Gel'mukhanov, F., and Ågren, H. (1999) Resonant X-ray Raman scattering. *Phys. Rep.*, **312** (3–6), 87–330.
113. Beye, M., Gühr, M., Hartl, I., Plönjes, E., Schaper, L., Schreiber, S., Tiedtke, K., and Treusch, R. (2023) FLASH and the FLASH2020+ project—current status and upgrades for the free-electron laser in Hamburg at DESY. *Eur. Phys. J. Plus*, **138** (3), 193.
114. Mukamel, S., Abramavicius, D., Yang, L., Zhuang, W., Schweigert, I.V., and Voronine, D.V. (2009) Coherent Multidimensional Optical Probes for Electron Correlations and Exciton Dynamics: From NMR to X-rays. *Acc. Chem. Res.*, **42** (4), 553–562.
115. Schweigert, I., and Mukamel, S. (2007) Probing valence electronic wave-packet dynamics by all x-ray stimulated Raman spectroscopy: A simulation study. *Phys. Rev. A*, **76** (1).
116. Kowalewski, M., Bennett, K., Dorfman, K.E., and Mukamel, S. (2015) Catching Conical Intersections in the Act: Monitoring Transient Electronic Coherences by Attosecond Stimulated X-Ray Raman Signals. *Phys. Rev. Lett.*, **115** (19), 193003.
117. Rohringer, N., Ryan, D., London, R.A., Purvis, M., Albert, F., Dunn, J., Bozek, J.D., Bostedt, C., Graf, A., Hill, R., Hau-Riege, S.P., and Rocca, J.J. (2012) Atomic inner-shell X-ray laser at 1.46 nanometres pumped by an X-ray free-electron laser. *Nature*, **481** (7382), 488–491.
118. Weninger, C., Purvis, M., Ryan, D., London, R., Bozek, J., Bostedt, C., Graf, A., Brown, G., Rocca, J., and Rohringer, N. (2013) Stimulated Electronic X-Ray Raman Scattering. *Phys. Rev. Lett.*, **111** (23), 233902.
119. Hillenkamp, F., Karas, M., Beavis, R.C., and Chait, B.T. (1991) Matrix-Assisted Laser Desorption/Ionization Mass Spectrometry of Biopolymers. *Anal. Chem.*, **63** (24), 1193A-1203A.
120. Fenn, J., Mann, M., Meng, C., Wong, S., and Whitehouse, C. (1989) Electrospray ionization for mass spectrometry of large biomolecules. *Science*, **246** (4926), 64–71.
121. Ueda, K., Sokell, E., Schippers, S., Aumayr, F., Sadeghpour, H., Burgdörfer, J., Lemell, C., Tong, X.-M., Pfeifer, T., Calegari, F., Palacios, A., Martin, F., Corkum, P., Sansone, G., Gryzlova, E.V., Grum-Grzhimailo, A.N., Piancastelli, M.N., Weber, P.M., Steinle, T., Amini, K., Biegert, J., Berrah, N., Kukk, E., Santra, R., Müller, A., Dowek, D., Lucchese, R.R., McCurdy, C.W., Bolognesi, P., Avaldi, L., Jahnke, T., Schöffler, M.S., Dörner, R., Mairesse, Y., Nahon, L., Smirnova, O., Schlathölter, T., Campbell, E.E.B., Rost, J.-M., Meyer, M., and Tanaka, K.A. (2019) Roadmap on photonic, electronic and atomic collision physics: I. Light–matter interaction. *J. Phys. B At. Mol. Opt. Phys.*, **52** (17), 171001.
122. Zettergren, H., Domaracka, A., Schlathölter, T., Bolognesi, P., Díaz-Tendero, S., Łabuda, M., Tosic, S., Maclot, S., Johnsson, P., Steber, A., Tikhonov, D., Castrovilli, M.C., Avaldi, L., Bari, S., Milosavljević, A.R., Palacios, A., Faraji, S., Piekarski, D.G., Rousseau, P., Ascenzi, D., Romanzin, C., Erdmann, E., Alcamí, M., Kopyra, J., Limão-Vieira, P., Kočišek, J.,

Fedor, J., Albertini, S., Gatchell, M., Cederquist, H., Schmidt, H.T., Gruber, E., Andersen, L.H., Heber, O., Toker, Y., Hansen, K., Noble, J.A., Jouvet, C., Kjær, C., Nielsen, S.B., Carrascosa, E., Bull, J., Candian, A., and Petrignani, A. (2021) Roadmap on dynamics of molecules and clusters in the gas phase. *Eur. Phys. J. D*, **75** (5), 152.

123. Calvert, C.R., Belshaw, L., Duffy, M.J., Kelly, O., King, R.B., Smyth, A.G., Kelly, T.J., Costello, J.T., Timson, D.J., Bryan, W.A., Kierspel, T., Rice, P., Turcu, I.C.E., Cacho, C.M., Springate, E., Williams, I.D., and Greenwood, J.B. (2012) LIAD-fs scheme for studies of ultrafast laser interactions with gas phase biomolecules. *Phys. Chem. Chem. Phys.*, **14** (18), 6289.

124. Calegari, F., Trabattoni, A., Palacios, A., Ayuso, D., Castrovilli, M.C., Greenwood, J.B., Decleva, P., Martín, F., and Nisoli, M. (2016) Charge migration induced by attosecond pulses in bio-relevant molecules. *J. Phys. B At. Mol. Opt. Phys.*, **49** (14), 142001.

125. Filsinger, F., Küpper, J., Meijer, G., Hansen, J.L., Maurer, J., Nielsen, J.H., Holmegaard, L., and Stapelfeldt, H. (2009) Pure Samples of Individual Conformers: The Separation of Stereoisomers of Complex Molecules Using Electric Fields. *Angew. Chem. Int. Ed.*, **48** (37), 6900–6902.

126. Johny, M., Onvlee, J., Kierspel, T., Bieker, H., Trippel, S., and Küpper, J. (2019) Spatial separation of pyrrole and pyrrole-water clusters. *Chem. Phys. Lett.*, **721**, 149–152.

127. Bieker, H., Onvlee, J., Johny, M., He, L., Kierspel, T., Trippel, S., Horke, D.A., and Küpper, J. (2019) Pure Molecular Beam of Water Dimer. *J. Phys. Chem. A*, **123** (34), 7486–7490.

AUTHOR BIOGRAPHIES

Dennis Mayer is currently a postdoctoral researcher at the FLASH free-electron laser at Deutsches Elektronen-Synchrotron DESY in Hamburg, Germany. He holds a master's degree in physics and a PhD in experimental physics from the University of Potsdam in Germany. His research focuses on the investigation of energy conversion mechanism of UV-excited biomolecules, particularly nucleobases and their analogs, using ultrafast x-ray pulses from free-electron lasers.

Fabiano Lever is a scientist at the Free Electron Laser FLASH. He obtained his master's in theoretical physics from the University of Trento and he completed his doctorate in experimental physics in the University of Potsdam. His research focuses on the mechanism of photoenergy conversions in small molecules, with a particular interest on thionucleobases. He specializes in ultrafast x-ray methods and data analysis techniques.

Markus Gühr is the head of the FLASH free-electron laser in the photon science department at the Deutsches Elektronen-Synchrotron (DESY) and professor of physical chemistry at the University of Hamburg. Markus Gühr's research interest lies in the energy conversion of (sun) light into other forms of energy in molecules, with a focus on the UV protection of

nucleobases. Markus Gühr uses X-ray and electron pulses to investigate the complex interplay between electrons and atomic nuclei in molecules during this conversion.